

BCI learning induces core-periphery reorganization in M/EEG multiplex brain networks

Marie-Constance Corsi^{a,b,*}, Mario Chavez^c, Denis Schwartz^d, Nathalie George^d, Laurent Hugueville^d, Ari E. Kahn^e, Sophie Dupont^b, Danielle S. Bassett^{e,f,g,h,i,j}, and Fabrizio De Vico Fallani^{a,b,*}

^aInria Paris, Aramis project-team, F-75013, Paris, France

^bInstitut du Cerveau et de la Moelle Epinière, ICM, Inserm, U 1127, CNRS, UMR 7225, Sorbonne Université, F-75013, Paris, France

^cCNRS, UMR 7225, F-75013, Paris, France

^dInstitut du Cerveau et de la Moelle Epinière, ICM, Inserm U 1127, CNRS UMR 7225, Sorbonne Université, Ecole Normale Supérieure, ENS, Centre MEG-EEG, F-75013, Paris, France

^eDepartment of Bioengineering, School of Engineering and Applied Science, University of Pennsylvania, Philadelphia, PA 19104, USA

^fDepartment of Neurology, Perelman School of Medicine, University of Pennsylvania, Philadelphia, PA 19104, USA

^gDepartment of Physics and Astronomy, College of Arts and Sciences, University of Pennsylvania, Philadelphia, PA 19104, USA

^hDepartment of Electrical and Systems Engineering, School of Engineering and Applied Science, University of Pennsylvania, Philadelphia, PA 19104, USA

ⁱDepartment of Psychiatry, Perelman School of Medicine, University of Pennsylvania, Philadelphia, PA 19104 USA

^jSanta Fe Institute, Santa Fe, NM 87501 USA

*Corresponding authors: Marie-Constance Corsi marie.constance.corsi@gmail.com; Fabrizio De Vico Fallani fabrizio.devicofallani@gmail.com

March 18, 2021

Abstract

Objective: Brain-computer interfaces (BCIs) constitute a promising tool for communication and control. However, mastering non-invasive closed-loop systems remains a learned skill that is difficult to develop for a non-negligible proportion of users. The involved learning process induces neural changes associated with a brain network reorganization that remains poorly understood.

Approach: To address this inter-subject variability, we adopted a multilayer approach to integrate brain network properties from electroencephalographic (EEG) and magnetoencephalographic (MEG) data resulting from a four-session BCI training program followed by a group of healthy subjects. Our method gives access to the contribution of each layer to multilayer network that tends to be equal with time.

Main results: We show that regardless the chosen modality, a progressive increase in the integration of somatosensory areas in the α band was paralleled by a decrease of the integration of visual processing and working memory areas in the β band. Notably, only brain network properties in multilayer network correlated with future BCI scores in the α_2 band: positively in somatosensory and decision-making related areas and negatively in associative areas.

Significance: Our findings cast new light on neural processes underlying BCI training. Integrating multi-modal brain network properties provides new information that correlates with behavioral performance and could be considered as a potential marker of BCI learning.

Introduction

Learning is a complex phenomenon that can be characterized by changes in regional associations and therefore in brain network organization [1]. Changes following learning have been revealed in language [2, 3] and in motor skill acquisition with resting-state fMRI recordings [4, 5]. In the case of motor learning, studies that focus on functional connectivity have demonstrated changes induced by skill acquisition [6, 7, 8, 9, 5]. From a network perspective, a large number of metrics characterizing network properties have been considered to capture the process of motor acquisition. In Ref. [10], the motor performance improvement was associated

with an increase of clustering coefficients, a higher number of network connections, an increased connection strength and shorter communication distances. Another approach consists of using a single metric that measures subnetwork segregation: modularity [11], already used as a marker of brain plasticity [12] and motor learning [13]. Motor skill acquisition induced an autonomy of sensorimotor systems and individual differences in the amount of learning could be predicted by the release of cognitive control hubs in frontal and cingulate cortices [14].

Mastering non-invasive closed-loop systems is a learned skill that requires several training sessions to achieve control of the device. Recent studies suggest that the involved learning process is analogous to cognitive or motor skill acquisition in the case of BCI [15]. It may induce behavioral modifications and neural changes within trained brain circuits in neurofeedback that last for several months after training [16]. Changes at the neuronal level, during the learning process, have also been observed and simulated [17]. The recruitment of areas beyond those targeted by BCI has been observed during skill acquisition [18, 19], and a decrease in the global efficiency index in the higher-beta frequency range with the practice of MI [20] suggests the involvement of a distributed core of brain areas while learning. From a theoretical perspective, the existence of a core, a group of tightly connected nodes, surrounded by a poorly connected periphery is crucial for the integration of information between remote network components [21, 22]. Previous studies have demonstrated the utility of using multilayer models of networks [23, 24] to study the relationship between structure and function in the human brain. The identification of core-periphery structures in brain networks can be significantly enriched by adding multiple levels of connectivity [25, 26]. In particular, combining multifrequency or multimodal neuroimaging data from a network perspective can reveal higher-order topological properties that cannot be detected by simple single-layer network approaches [27, 28, 29, 25, 30, 31, 32]. Magnetoencephalography (MEG) and electroencephalography (EEG) are complementary in terms of sensitivity towards source depths and conductivity, but also in terms of dipole orientation detection [33, 34, 35, 36, 37, 38]. As a result, their combination could provide valuable information, and has proven to enhance subjects' mental state discrimination in BCI [39].

On the above mentioned elements, we hypothesized that integrating information from EEG and MEG data, allow a better description of the core-periphery changes occurring during a motor imagery-based BCI training in a group of healthy subjects. Such an enriched description could reveal fresh insights into learning processes that are difficult to observe at the single layer level and eventually improve the prediction of future BCI performance.

Materials and Methods

Participants and experiment

We included twenty healthy, and BCI naive, subjects (aged 27.5 ± 4.0 years, 12 men). All right-handed, they participated in a 4 session-based BCI training during two weeks. According to the declaration of Helsinki, a written informed consent was obtained from subjects after explanation of the study, which was approved by the ethical committee CPP-IDF-VI of Paris. The EEG-based BCI consisted of a two-target box task [40]. The subjects were instructed to control the vertical position of a moving cursor by modulating the neural activity in the α [8-12 Hz] and/or β [14-29 Hz] frequency bands. Each session was divided into two phases:

1. The training phase consisted of five consecutive runs, of 32 trials each, without any feedback. For a given trial, the first second consisted of the inter-stimulus interval (ISI) followed by five seconds of target presentation. To elicit the (EEG electrodes; frequency bins) couples that best discriminate the subjects' mental state over the left motor area and within the mu-beta frequency ranges, we computed contrast maps that relied on the R-square metric [41].
2. The testing phase consisted of six runs, of 32 trials each, with a cursor feedback. Similarly to the training phase, for a given trial, we had one second of ISI, while the target was presented throughout the subsequent five seconds. The visual feedback, displayed from $t = 3s$ to $t = 6s$, consists of a moving cursor. The features, i.e. power spectra estimated at the (EEG electrodes; frequency bins) couples selected during the training, were classified by using the Linear Discriminant Analysis method. All the results presented in the following sections relied on the analysis performed on the testing data.

To perform the experiments, we used a 74 EEG-channel system, with Ag/AgCl passive sensors (Easycap, Germany) placed according to the standard 10-10 montage. The reference was located at the mastoids and the ground electrode was placed at the left scapula. We kept the impedances lower than 20 kOhms. The MEG system consisted of 102 magnetometers and 204 gradiometers (Elekta Neuromag TRIUX MEG system). E/MEG registrations were performed simultaneously in a magnetic shielded room with a sampling frequency of 1 kHz and a bandwidth of 0.01-300 Hz. The subjects were seated with palms facing upward in front of a 90 cm-distant screen. To ensure that no forearm movements were performed, experts visually inspected electromyogram (EMG) signals recorded from the subject's right arm during the experiment. During the sessions, BCI feedback relied on EEG signals transmitted to the BCI2000 toolbox [41] via the Fieldtrip buffer [42]. Individual T1 sequences have been obtained by using a 3T Siemens Magnetom PRISMA

after the fourth session to ensure accurate head models [43]. These registrations consisted of a 15 minute-resting-state task. A preprocessing of the images was performed via the FreeSurfer toolbox [44] and directly imported (15002 vertices) to the Brainstorm toolbox. To provide co-registration with the anatomical MRI, we digitized the location of the EEG electrodes and three landmarks (nasion, left and right pre-auricular points) with the FastTrak 3D digitizer (Polhemus, Inc., VT, USA). These locations were aligned with the MRI using the Brainstorm toolbox [45]. A more detailed description of the experiments is proposed in Ref. [46].

Data analysis

M/EEG processing

After a first preprocessing step that consisted of an application of the temporal extension of the Signal Space Separation (tSSS) to MEG signals to remove environmental noise [47], M/EEG data were downsampled to 250 Hz and processed via the Independent Component Analysis [48, 42] to remove ocular and cardiac artifacts. Then, data were segmented into 7s-epochs, corresponding to the trial length.

Source reconstruction was performed by applying the Boundary Element Method [49, 50] to obtain the individual head model, followed by the estimation of the sources with the weighted Minimum Norm Estimate [51, 52, 53, 45]. A more detailed description of the applied preprocessing steps is proposed in Ref. [46].

To compute the power spectra within the individual anatomical space, we used the Welch method. A time window of 1 s and a window overlap ratio of 50 % was applied during the feedback period (i.e. from $t = 3$ s to $t = 6$ s) to obtain the cross-spectral estimation for each trial, session, and subject. Then, for each region of interest (ROI) from the Destrieux atlas [54], we took into account the first principal component of the power spectra computed over the dipoles. For each layer (or modality here) l and frequency band f , we estimated the functional connectivity networks by computing the imaginary coherence between each pair of ROIs ($N = 148$) [55], resulting in 148×148 adjacency matrices $A_{l,f}$.

Network analysis and statistics

Similarly to Refs [26, 32], to obtain the multilayer or multiplex brain networks M_f for a given frequency band f from the adjacency matrices $A_{l,f}$, we aligned the EEG and MEG connectivity networks as follows:

$$M_f = A_{l,f}, \forall l \in \{EEG, MEG\}, \quad (1)$$

To study properties associated with a core-periphery organization, for a given layer (i.e. modality here), we filtered the associated adjacency matrix $A_{l,f}$ to keep the strongest weights by applying a broad range of thresholds corresponding to the average node degree $k = 1$ to $k = N - 1$. For each threshold k , to determine whether a node i belongs to the core, we computed the multiplex core-periphery of the filtered network by calculating its richness defined as follows:

$$\mu_i = \sum_{l=1}^L c^l s_i^l, \quad (2)$$

where L corresponds to the number of layers ($L = 2$), s_i^l corresponds to the strength of the node i in the l -th layer (i.e. the sum of the i -th row of the matrix $A_{l,f}$), and c^l corresponds to the l -th component of the vector c that represents the contribution of each layer (ranging from 0 to 1). To take into account only the links of node i that are associated with nodes of higher richness, we decomposed the richness function as follows: $s^l = s^{l-} + s^{l+}$. The richness of nodes linked to richer nodes can be defined as:

$$\mu_{i+} = \sum_{l=1}^L c^l s_i^{l+}. \quad (3)$$

We finally computed the multiplex coreness [26] C_i of each node i , independently from any other consideration, by determining the number of times the node i belongs to the core over all the k tested thresholds, as follows:

$$C_i = \frac{1}{N-1} \sum_{k=1}^{N-1} \delta_i^k, \quad (4)$$

where $\delta_i^k = 1$ if node i belongs to the core for the threshold k , and 0 otherwise. To obtain the coreness associated with a specific layer, one can simply modify the vector c in equation 3 so that the component not related to the given modality is equal to zero. For each subject, session and frequency band, we optimized the choice of the components of the vector c by using the Particles Swarm Optimization and Statistical Analysis (PSO) algorithm [32, 56]. In our case, the Fisher's criterion $F(c)$, chosen to maximize the difference between the conditions, was defined as follows:

$$F(c) = \frac{(\langle C^{MI}(c) \rangle - \langle C^{rest}(c) \rangle)^2}{(s^{MI})^2 + (s^{rest})^2}, \quad (5)$$

where $\langle C^{cond}(c) \rangle$ is the averaged coreness computed over the nodes i in the condition $cond$ and

$$(s^{cond})^2 = \sum_{i \in \{1..N\}} (C_i^{cond}(c) - \langle C^{cond}(c) \rangle)^2, \quad (6)$$

where C_i^{cond} corresponds to the coreness computed in node i in the condition $cond$.

To study the variation of coreness between conditions, we defined the relative coreness (ΔC) as $\Delta C = C^{MI} - C^{Rest}$. To compute the multiplex core-periphery properties, we used the Brain Connectivity Toolbox [57] and the Matlab code available at <https://github.com/brain-network/bnt>.

To take into account the subjects' specificity, we used customized definitions of the α and β bands [58], that rely on the Individual Alpha Frequency (IAF) [59], obtained from a 3-minute resting state recording. The α_1 ranges from IAF - 2 Hz to IAF, α_2 from IAF to IAF + 2 Hz, β_1 from IAF + 2 Hz to IAF + 11 Hz and β_2 from IAF + 11 Hz to IAF + 20 Hz. Preliminary results did not show particularly significant effects in θ and low γ bands. Therefore, only results obtained within the α and β frequency bands are presented here.

After plotting quantile-quantile plots and performing the Shapiro-Wilk test [60], it became clear that the coreness values were not normally distributed. Thus, to evaluate the session and the modality effect on the coreness and its associated properties, we fitted and tested an ANOVA using 5000 permutation-tests (ImPerm package in R). Correlations between BCI scores and coreness were estimated via the use of repeated-measures correlations (rmcorr package in R [61]).

Results obtained from paired t -tests between conditions (to assess the condition effect) and from repeated-measures correlations referred to a statistical threshold of 0.05 corrected for multiple comparisons by adopting a false discovery rate (FDR) criterion [62], which is a method extensively used in biological studies [63, 64, 65].

Results

Before studying the evolution of network properties over sessions, we first determined whether a learning effect was actually present. We applied a one-way repeated non-parametric ANOVA on the BCI accuracy scores averaged across the runs of each session with the session number as the intra-subject factor (Figure 1A). Results confirmed that a learning effect was present at the group level ($F(3, 57) = 13.9$, $p = 6.56 \cdot 10^{-7}$). In particular, sixteen subjects out of 20 achieved the ability to control the moving cursor by the end of the training, with accuracy scores above the chance level of 57% [66].

As explained in the previous section, we started our analysis by using the adjacency matrices obtained from [46] to build single layer networks (Figure 1B, see Supplementary Materials *Figures S1 & S2*), and we investigated in which extent integrating the network properties obtained from EEG and MEG would be beneficial to the search of BCI training markers.

As a preliminary step, we studied the evolution of the attributed weights across sessions (Figure 1C, see

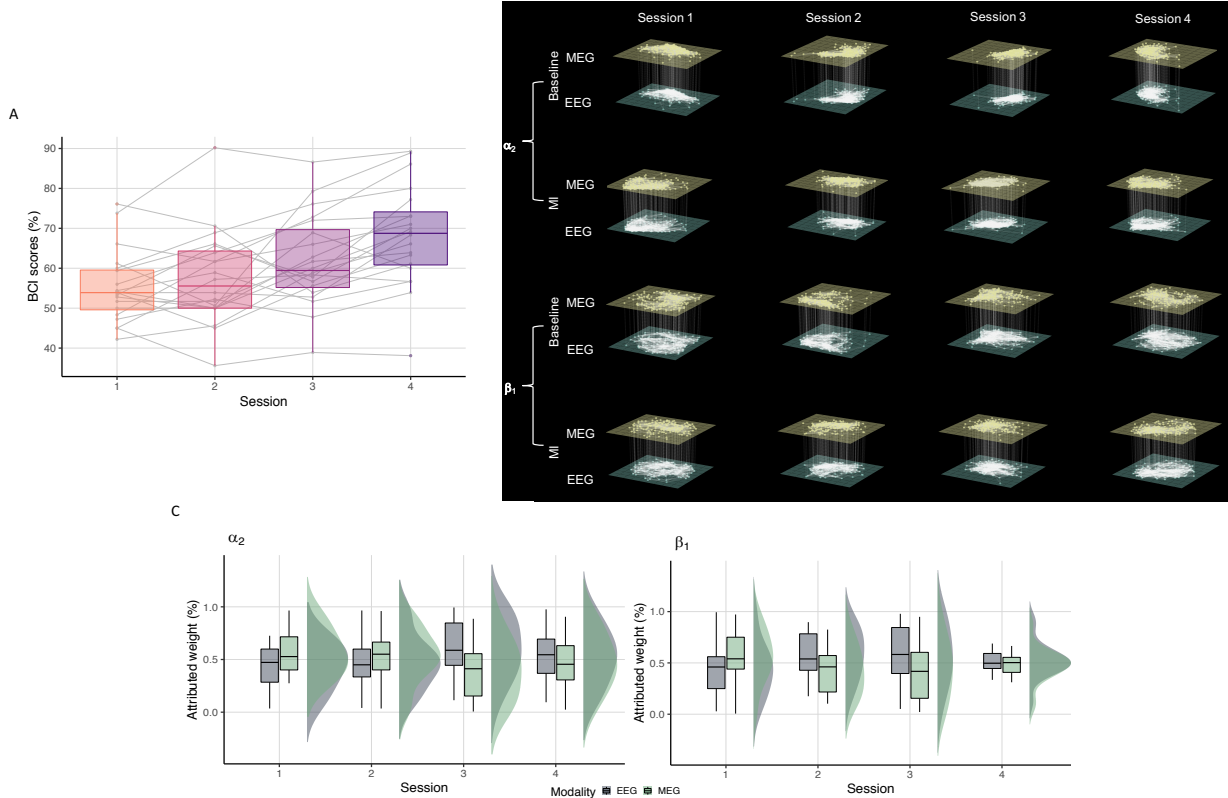


Figure 1: Behavioral performance and E/MEG contributions. (A) Distribution of BCI accuracy scores averaged across the runs of each session. Horizontal lines inside the box represent the median values. (B) Evolution of the E/MEG networks over sessions (average over the participants), obtained for each session, and condition within the α_2 (top) and β_1 (bottom) ranges. (C) Evolution of attributed weights over sessions within the α_2 (top) and β_1 (bottom) ranges. We plotted in grey and green the weight distribution associated, respectively, with EEG and MEG. Horizontal lines inside the box represent the median values.

Supplementary Materials *Figure S3*). We observed that the main session and modality effects occurred within the α and the β bands, with significant interaction effects in α_2 and β_1 bands (two-way ANOVA, respectively $p=0.022$ and $p=0.027$). In these bands, we observe similar trends. In session 1, w_{MEG} is larger than w_{EEG} ; then, the opposite effect occurred before the convergence to 0.5 at session 4. This final convergence to 0.5 indicates a progressive equal contribution of the two modality layers on the regional multiplex coreness.

Multiplex core-periphery provides additional information

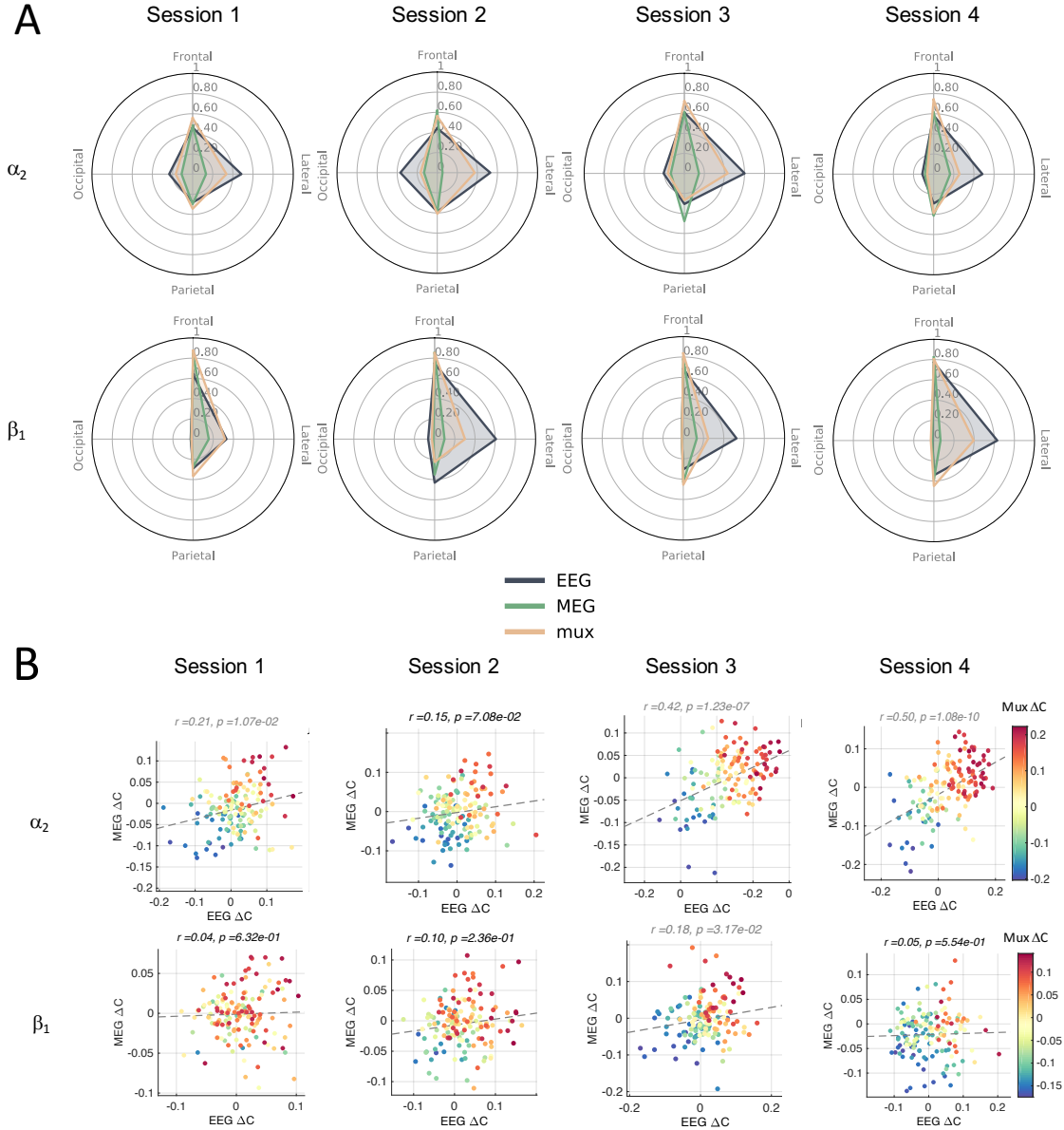
We studied single and multiplex (mux) coreness trends over sessions in the MI condition (Figure 2A). Similar tendencies were observed in the different modalities both within the α and β frequency ranges (see Supplementary Materials *Figure S4*). In particular, we observed that the highest values of MI coreness were

obtained in ROIs that belongs to the frontal lobe. In α_2 , we obtained a progressive increase of the median value within the frontal lobe, especially in mux (see Figure 2A). The second most important lobe was the lateral one, in particular for EEG and mux. We noticed an increase of the median value obtained within parietal lobe in MEG. In β_1 , these observations were even clearer with an increase of the values obtained within the lateral lobes in EEG and mux, whereas values within in the parietal lobe were stable and those obtained within the occipital lobe were negligible. These first observations showed that specific brain lobes presented clear variations of coreness values depending on the considered modality (for a more detailed presentation of the distribution of coreness values in the MI condition, see Supplementary Materials *Figure S5*, and for a presentation of multiplex coreness values, see and Supplementary Materials *Figure S6*).

The scatter plots represented in (Figure 2B) are associated with the relative coreness (ΔC) values obtained for each single layer (X and Y axis) and also for the multiplex. Within the α band, we observed that the distribution of points progressively followed a linear relationship between EEG and MEG ΔC values, meaning a non-negligible part of the information is shared by these modalities at the end of the training. Within the β band, we noticed an absence of a linear relationship between EEG and MEG, meaning that the two single layers shared less common information.

Furthermore, we assessed the modality effect associated with ΔC via a one-way ANOVA, with the modality taken as the intra-subject factor. In the $\alpha - \beta$ ranges the parahippocampal gyrus significantly differed between modalities ($p < 0.030$) associated with visual functions [67]. Within the α frequency range, we observed a significant modality effect in the middle-anterior part of the cingulate gyrus ($p < 0.030$) involved during decision making and memory consolidation [68]. In the β_1 band, the long insular gyrus, also associated with decision making [69] presented a significant difference in terms of modality ($p < 0.001$). The presented modality effects were driven by a significant difference between EEG and MEG relative coreness (Tukey *post - hoc* multiple pairwise comparisons, p -values adjusted via the Holm method $p < 0.050$).

We also evaluated the information of interest provided by the multiplex with respect to single layers by statistically comparing the coreness of the MI versus the Rest conditions with a paired t-test ($p < 0.021$, see Supplementary Materials *Tables S1-S3*). We observed two opposite trends depending on the frequency range. In α_2 , at the single layer level, no consistent significant ROIs were obtained whereas we observed an increased involvement of the gyrus rectus with the multiplex with the training ($p < 0.01$ at session 4). This brain area is known to be associated with decision making involving a reward [70]. Within the β ranges, we observed a lower number of ROIs showing a significant condition effect. In β_1 , at the single



layer, no significant ROIs ($p < 0.021$) were obtained during the first session whereas the multiplex presented three: short insular gyri (involved in motor planning [69]), planum polare of the superior temporal gyrus (deductive reasoning [71]), and the gyrus rectus (see Supplementary Materials *Table S3*).

In the next sections, to directly account for the variations of coreness between conditions, we will focus our study on the relative coreness ΔC . Furthermore, in order to take into account the most informative ROIs, we pre-selected the areas that show a significant condition effect at least once during the training before performing the analysis presented in the subsequent sections.

Relative coreness changes during training

To provide a more detailed description of the evolution of the relative coreness over training, we performed a one-way ANOVA for each layer separately (see Supplementary Materials *Figures S8*).

We observed that ΔC presented a significant session effect involving different brain areas (Figure 3A, see Supplementary Materials *Figure S7*). Within the α_2 range, a significant session effect was observed in EEG mostly within the long insular gyrus and the gyrus rectus; a significant session effect was observed in MEG in the supramarginal gyrus (working memory and motor planning [72]); and in the multiplex a significant session effect was observed in areas involved during motor planning and working memory (orbital part of the inferior frontal gyrus and subcallosal gyrus) [73, 74, 75] and in learning complex motor skills (middle-posterior part of the cingulate gyrus)[76]. In each case, we obtained an increase of ΔC with training (see Figure 3A and Supplementary Materials *Figure S7*).

Within the β_1 range, a significant session effect was observed in EEG within the inferior temporal gyrus (dual working memory task processing) and in the multiplex in areas associated with visual processing (superior temporal gyrus), working memory (middle frontal gyrus), and motor planning (short insular gyri). In the multiplex, most of the ROIs showing a significant session effect present a decrease of ΔC with training (see Figure 3B).

Multiplex relative coreness correlated with future BCI performance

For the sake of simplicity, we will present our results only with relative coreness within the α_2 band where the most significant observations were made. For a complete presentation of the results, see Supplementary Materials *Figure S10-S11*.

We observed that the relative coreness presents a significant correlation with the BCI scores, within a larger number of significant ROIs in the multiplex in comparison with EEG or MEG (see Supplementary Materials

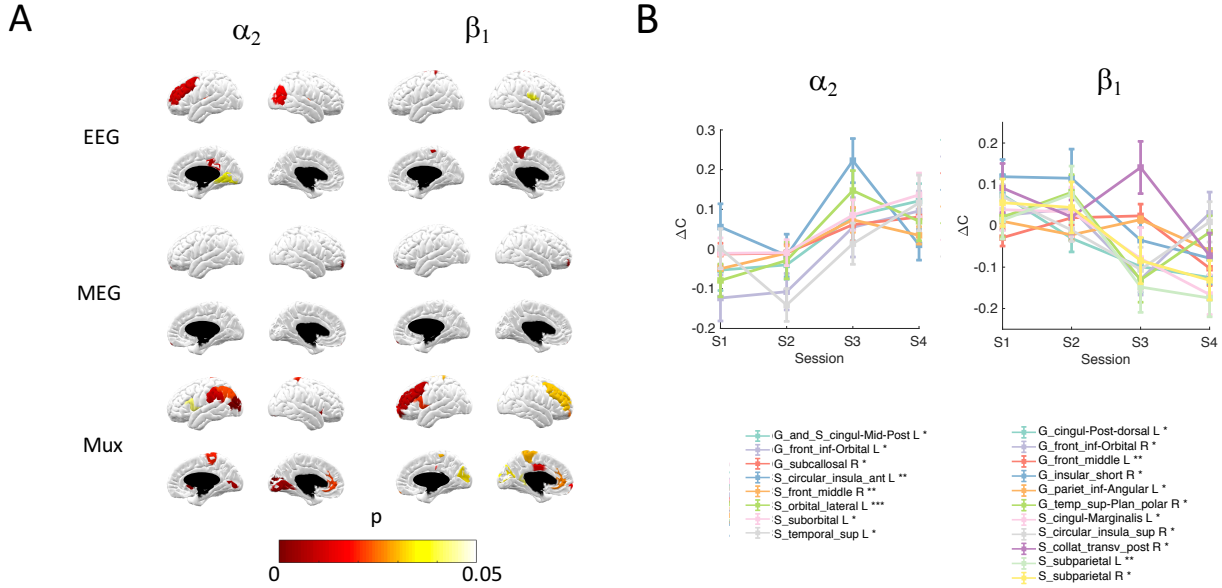


Figure 3: Relative coreness changes during training. (A) ROIs showing a significant session effect (one-way ANOVA, $p < 0.05$). (B) Distribution over the training in the multiplex. Only the ROIs that present a significant session effect are represented (one-way ANOVA, $p < 0.05^*$, $p < 0.01^{**}$, $p < 0.001^{***}$).

Figure S10). In EEG, negative correlations were obtained within the posterior-ventral part of the cingulate gyrus, the fronto-marginal gyrus ($p < 0.01$) (respectively involved during learning a complex motor skill and working memory [76, 77, 78, 79]) and a positive correlation within the middle temporal gyrus (involved during the observation of motion [80]). In MEG, a positive correlation was observed within the triangular part of the inferior frontal gyrus ($p < 0.01$, involved during motor response inhibition and working memory [73, 74, 75]) and a negative correlation within the cuneus (involved during visual processing [81]). In the multiplex networks, positive correlations were obtained in regions involved respectively during motor tasks and motor imagery with working memory tasks (subcentral gyrus, superior parietal lobule, and subcallosal gyrus) [82, 79, 83, 7]. A negative correlation was obtained within the gyrus rectus (decision making involving reward).

To assess whether relative coreness could be associated with future BCI performance, we estimated the correlation between ΔC in session i and the BCI score obtained in session $i + 1$. We observed significant correlations only with multiplex within the α_2 band (Figure 4). More precisely, a positive correlation ($p < 0.01$) was observed in the gyrus rectus, the subcentral gyrus, but also the long insular gyrus (involved during somatosensory tasks [69]). A negative correlation was obtained in the superior occipital gyrus associated

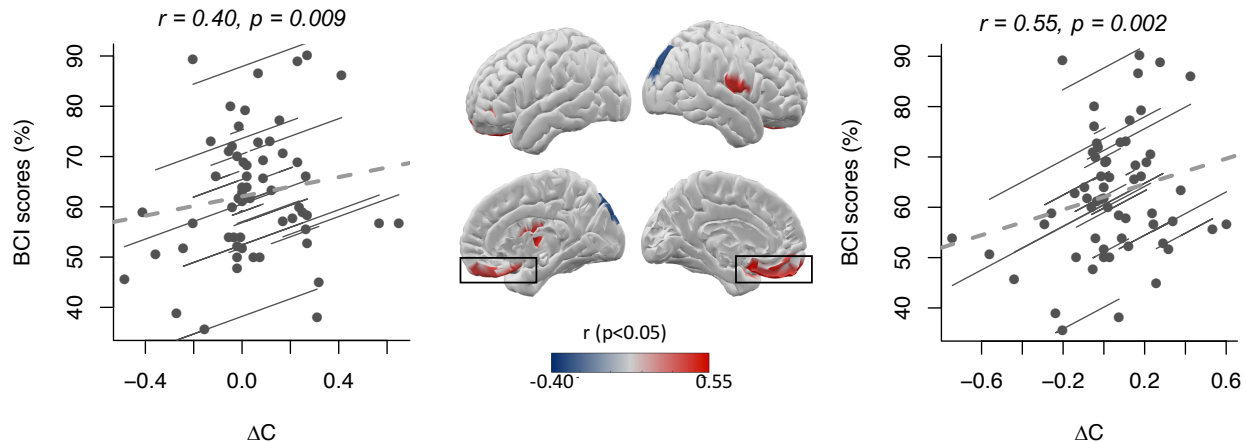


Figure 4: Repeated correlations between BCI performance of the subsequent session and the multiplex relative coreness in the alpha2 band. At the center, we plotted the r-values projected onto the scalp ($p < 0.05$). On either side, scatter plots obtained from the two ROIs showing the highest r-values ($p < 0.01$). The dashed line represents the overall regression plot and the paralleled lines correspond to the fit to each subject’s data taken separately.

with visual processing (in blue in Figure 4) [84].

Discussion

Controlling a BCI remains a learned skill that is difficult to develop for a non-negligible number of users (15 % - 30 %) [85]. Previous studies dedicated to elicit neural dynamics underlying BCI skill acquisition in primates [86, 87] and humans [20, 19] suggest the presence of a distributed and dynamic network of cortical areas above the motor-related ones. However, the evolution of such brain networks over training is largely unknown mainly because of a lack of longitudinal studies based on BCI paradigms [88]. Our protocol relied on reinforcement learning [89] based on a well-known two-target box task [40] where a training effect has been obtained. In this study, we were particularly interested in understanding the brain network macroscale changes during the learning process. A few number of works, relying on BCI protocols and involving healthy subjects, have previously addressed this question [46, 90].

Tracking core-periphery changes

It has been proved that core-periphery properties could be a valuable tool to track brain reorganization associated with cognitive processes [91] but also disorders [92, 93]. In this study, we worked with the coreness, a concise and robust metric that enables us to assess the likelihood to belong to the core of a network [25, 26]. Regardless of the modality, opposite trends were obtained within the α and β ranges

in terms of the evolution of the discrimination between conditions and of the ΔC values with time (see Supplementary Materials *Figure S8* and *Tables S1-S3*). Nevertheless, these observations were particularly true for the multiplex involving α_2 areas associated with somatosensory tasks and motor planning, and β_1 in areas associated with visual processing and working memory (see *Figure 3*).

The α activity is known to be linked to the inhibition of task-irrelevant areas [94, 95, 96]. If β desynchronization is clearly associated with sensorimotor tasks, recent studies suggest that β -synchrony maintains the current sensorimotor set [97, 98]. In addition, β activity is implicated in specific functions such as visual perception [99, 100] and working memory [101], and is associated with top-down controlled processing [98]. From a functional connectivity perspective, in a previous work, we showed that MI-based BCI learning was associated with a progressive decrease of node strength in associative cortical regions and with the reinforcement of sensorimotor activity targeted by the experiment [46]. In this case, α_2 and β_1 shared a common behaviour. Altogether, these results suggest a joint response of α_2 with β_1 frequency bands during BCI training, associated with a reinforcement of the integration of sensorimotor areas in α_2 paralleled with a functional connectivity release in the associative areas involved during visual processing and working memory in β_1 .

Layer comparisons

The complementary role of EEG and MEG has been proved at different levels: dipole orientation and source localization [36, 38, 102] and subjects' mental state classification [39]. However, such complementarity has been poorly studied at the network level despite some interesting results in functional connectivity [103]. To better capture network changes at different time or spatial scales, one can use multilayer models of networks [23, 24]. This approach enabled for example, in the time domain, to predict the relative learning rate via the flexibility [13] in motor skill acquisition, but also to identify core-periphery changes in Alzheimer disease via a multimodal approach combining structural and functional networks [25, 26, 32].

Here, based on previous work where MEG and DTI were combined [32], we integrated modalities knowing the contribution of each of them in such a way as to ensure the highest separation between conditions. These weights tended to converge to 0.5 (see *Figure 1C*), meaning that the two modalities provided similar contribution to the multiplex network towards the end of the BCI training. This finding suggests that the two modalities are as important to discriminate MI and Rest conditions in the multiplex at the end of the training. As a result, the multiplex appeared to present a larger and more robust condition effect with respect to EEG and MEG (see Supplementary Materials *Figures S7* and *Tables S1-S3*). However, the attributed

weights did not present a significant correlation with BCI performance. The approach proposed here also raised the possibility to compare results obtained from different layers. In particular, in α_2 , we obtained a progressive linear relationship between EEG and MEG relative corenesses with time over all the ROIs (see Figure 2B). This result suggests that, at a global level, MEG and EEG capture similar task-related processes occurring during the BCI experiment, especially at the end of training. The modality effects, suggested in Figure 2A, and actually observed at the relative coreness level, were driven by a significant difference between EEG and MEG relative corenesses. This effect was mostly observed in areas associated with decision making and memory consolidation, highlighting the utility to combine MEG and EEG networks to better capture mechanisms underlying learning process.

Markers of cognitive performance

Identifying neural features underlying BCI performance is crucial to design optimized and individualized BCI architectures [104, 105]. Among the elicited markers are psychological and demographical traits [106]. From a neurophysiological perspective, previous studies identified power spectra in θ , α and γ bands as potential predictors of BCI scores [107, 108]. In our study, the most significant results were obtained in α_2 and β_1 frequency bands. Recent findings proved that functional connectivity could correlate with the user's performance [109, 59, 110]. However, these studies were associated with a single session BCI performance. In a recent work, we showed that the regional connectivity strength of specific associative cortical areas could explain the BCI performance in the same session but also the future learning rate [46]. Here, we were particularly interested in identifying markers of BCI performance at the core-periphery network level.

If EEG, MEG, and multiplex presented associations with BCI scores, only the latter presents a significant correlation with the BCI performance of the next session based on the relative coreness within the α_2 band (see Supplementary Materials *Figure S10-S11*). Two trends were again observed: a positive correlation in areas respectively involved during decision making and somatosensory tasks (gyrus rectus, subcentral gyrus, and long insular gyrus) and a negative correlation in the superior occipital gyrus associated with visual processing (see Figure 4). These findings are in line with previous studies that reported a larger clustering coefficient in the gyrus rectus associated with a higher nodal betweenness centrality (NBC) in sensorimotor areas and a reduced NBC in visual areas in the context of motor training [111, 112]. Altogether, these results support the hypothesis that sensorimotor areas and associative areas play a crucial role in motor sequence learning as well as in abstract task learning [7, 113, 114, 115] and that cognitive processes involved in the supervisory attentional system [116, 117] are important to perform MI tasks [118] and motor learning

[119, 120, 121, 122].

Caveats and perspectives

The temporal window of study is a crucial matter when considering a longitudinal experimentation, especially in the BCI domain. Our participants followed a four-session-training program, within two weeks. This temporal window might not be sufficient to observe the full learning process [123, 88]. However our results constitute the first observations of a training process at the core-periphery level. Further studies based on longer BCI training are necessary to assess whether our observations could be still verified on a larger temporal scale.

This work could pave the way to further explore of the integration of M/EEG network information to better understand neural mechanisms underlying learning but also task performance in particular in the use of BCI in a clinical context. However, before considering multimodal BCIs in routine, further developments are required to increase MEG portability. The use of new generation of MEG sensors (i.e. optically-pumped magnetometers) could meet this need [124, 125, 126, 127].

Conclusion

In this work, we have proved that studying the network integration changes at the single and multilayer levels provides additional information to characterize dynamic brain reorganization during BCI training. We found that a progressive increase of the integration of somatosensory areas in the α band was paralleled by a decrease of the integration of visual processing and working memory areas in the β band. More importantly, these changes were more visible in multiplex in which brain network properties correlated with future BCI scores in the α_2 band. Taken together, our results cast new light on brain network reorganization occurring during BCI training and more generally during human learning.

References

- [1] Reddy, P. G. *et al.* Brain state flexibility accompanies motor-skill acquisition. *Neuroimage* **171**, 135–147 (2018). URL <http://www.sciencedirect.com/science/article/pii/S1053811917311175>.
- [2] Deng, Z., Chandrasekaran, B., Wang, S. & Wong, P. C. Resting-state low-frequency fluctuations reflect individual differences in spoken language learning. *Cortex* **76**, 63–78 (2016). URL <https://www.ncbi.nlm.nih.gov/pmc/articles/PMC4777637/>.

- [3] Sheppard, J. P., Wang, J.-P. & Wong, P. C. M. Large-scale Cortical Network Properties Predict Future Sound-to-Word Learning Success. *Journal of Cognitive Neuroscience* **24**, 1087–1103 (2012). URL <https://www.ncbi.nlm.nih.gov/pmc/articles/PMC3736731/>.
- [4] Sami, S. & Miall, R. C. Graph network analysis of immediate motor-learning induced changes in resting state BOLD. *Frontiers in Human Neuroscience* **7** (2013). URL <https://www.ncbi.nlm.nih.gov/pmc/articles/PMC3654214/>.
- [5] Taubert, M., Lohmann, G., Margulies, D. S., Villringer, A. & Ragert, P. Long-term effects of motor training on resting-state networks and underlying brain structure. *Neuroimage* **57**, 1492–1498 (2011). URL <https://doi.org/10.1016/j.neuroimage.2011.05.078>.
- [6] Ge, R., Zhang, H., Yao, L. & Long, Z. Motor imagery learning induced changes in functional connectivity of the default mode network. *IEEE Transactions on Neural Systems and Rehabilitation Engineering* **23**, 138–148 (2015). URL <https://ieeexplore.ieee.org/document/6849455>.
- [7] McDougle, S. D., Ivry, R. B. & Taylor, J. A. Taking Aim at the Cognitive Side of Learning in Sensorimotor Adaptation Tasks. *Trends in Cognitive Sciences* **20**, 535–544 (2016). URL <http://dx.doi.org/10.1016/j.tics.2016.05.002>.
- [8] Rizzolatti, G. & Luppino, G. The cortical motor system. *Neuron* **31**, 889–901 (2001). URL [http://dx.doi.org/10.1016/s0896-6273\(01\)00423-8](http://dx.doi.org/10.1016/s0896-6273(01)00423-8).
- [9] Katiuscia, S. *et al.* Reorganization and enhanced functional connectivity of motor areas in repetitive ankle movements after training in locomotor attention. *Brain Research* **1297**, 124–134 (2009). URL <http://www.sciencedirect.com/science/article/pii/S0006899309017661>.
- [10] Heitger, M. H. *et al.* Motor learning-induced changes in functional brain connectivity as revealed by means of graph-theoretical network analysis. *Neuroimage* **61**, 633–650 (2012). URL <https://doi.org/10.1016%2Fj.neuroimage.2012.03.067>.
- [11] Sporns, O. & Betzel, R. F. Modular Brain Networks. *Annual Review of Psychology* **67**, 613–640 (2016). URL <http://dx.doi.org/10.1146/annurev-psych-122414-033634>.
- [12] Gallen, C. L. & D’Esposito, M. Brain Modularity: A Biomarker of Intervention-related Plasticity. *Trends in Cognitive Sciences* (2019). URL <http://www.sciencedirect.com/science/article/pii/S1364661319300427>.

- [13] Bassett, D. S. *et al.* Dynamic reconfiguration of human brain networks during learning. *Proceedings of the National Academy of Sciences of the United States of America* **108**, 7641–7646 (2011). URL <http://www.ProceedingsoftheNationalAcademyofSciencesoftheUnitedStatesofAmerica.org/content/108/18/7641>.
- [14] Bassett, D. S., Yang, M., Wymbs, N. F. & Grafton, S. T. Learning-induced autonomy of sensorimotor systems. *Nature Neuroscience* **18**, 744–751 (2015). URL <http://dx.doi.org/10.1038/nn.3993>.
- [15] Hiremath, S. V. *et al.* Brain computer interface learning for systems based on electrocorticography and intracortical microelectrode arrays. *Frontiers in Integrative Neuroscience* **40** (2015). URL <http://dx.doi.org/10.3389/fnint.2015.00040>.
- [16] Sitaram, R. *et al.* Closed-loop brain training: the science of neurofeedback. *Nature Reviews Neuroscience* **18**, 86–100 (2016). URL <https://doi.org/10.1038/nrn.2016.164>.
- [17] Ito, H., Fujiki, S., Mori, Y. & Kansaku, K. Self-reorganization of neuronal activation patterns in the cortex under brain-machine interface and neural operant conditioning. *Neuroscience Research* (2020). URL <http://dx.doi.org/10.1016/j.neures.2020.03.008>.
- [18] Orsborn, A. L. & Pesaran, B. Parsing learning in networks using brain-machine interfaces. *Current Opinion in Neurobiology* **46**, 76–83 (2017). URL <http://dx.doi.org/10.1016/j.conb.2017.08.002>.
- [19] Wander, J. D. *et al.* Distributed cortical adaptation during learning of a brain-computer interface task. *Proceedings of the National Academy of Sciences of the United States of America* **110**, 10818–10823 (2013). URL <https://doi.org/10.1073/pnas.1221127110>.
- [20] Pichiorri, F. *et al.* Sensorimotor rhythm-based brain-computer interface training: the impact on motor cortical responsiveness. *Journal of Neural Engineering* **8**, 025020 (2011). URL <http://dx.doi.org/10.1088/1741-2560/8/2/025020>.
- [21] Borgatti, S. P. & Everett, M. G. Models of core/periphery structures. *Social Networks* **21**, 375–395 (2000). URL <http://www.sciencedirect.com/science/article/pii/S0378873399000192>.
- [22] Girvan, M. & Newman, M. E. J. Community structure in social and biological networks. *Proceedings of the National Academy of Sciences of the United States of America* **99**, 7821–7826 (2002).

- URL <https://www.ProceedingsoftheNationalAcademyofSciencesoftheUnitedStatesofAmerica.org/content/99/12/7821>. Publisher: National Academy of Sciences Section: Physical Sciences.
- [23] De Domenico, M. *et al.* Mathematical Formulation of Multilayer Networks. *Physical Review X* **3**, 041022 (2013). URL <https://link.aps.org/doi/10.1103/PhysRevX.3.041022>.
- [24] Boccaletti, S. *et al.* The structure and dynamics of multilayer networks. *Physics Reports* **544**, 1–122 (2014). URL <http://www.sciencedirect.com/science/article/pii/S0370157314002105>.
- [25] Battiston, F., Nicosia, V., Chavez, M. & Latora, V. Multilayer motif analysis of brain networks. *Chaos: An Interdisciplinary Journal of Nonlinear Science* **27**, 047404 (2017). URL <https://aip.scitation.org/doi/10.1063/1.4979282>.
- [26] Battiston Federico, Guillon Jeremy, Chavez Mario, Latora Vito & De Vico Fallani Fabrizio. Multiplex core–periphery organization of the human connectome. *Journal of The Royal Society Interface* **15**, 20180514 (2018). URL <https://royalsocietypublishing.org/doi/full/10.1098/rsif.2018.0514>.
- [27] De Domenico, M., Sasai, S. & Arenas, A. Mapping Multiplex Hubs in Human Functional Brain Networks. *Frontiers in Neuroscience* **10** (2016). URL <https://www.ncbi.nlm.nih.gov/pmc/articles/PMC4945645/>.
- [28] De Domenico, M. Multilayer modeling and analysis of human brain networks. *Gigascience* **6**, 1–8 (2017). URL <https://www.ncbi.nlm.nih.gov/pmc/articles/PMC5437946/>.
- [29] Tewarie, P. *et al.* Integrating cross-frequency and within band functional networks in resting-state MEG: A multi-layer network approach. *Neuroimage* **142**, 324–336 (2016). URL <http://dx.doi.org/10.1016/j.neuroimage.2016.07.057>.
- [30] Guillon, J. *et al.* Loss of brain inter-frequency hubs in Alzheimer’s disease. *Scientific Reports* **7** (2017). URL <https://www.nature.com/articles/s41598-017-07846-w>.
- [31] Buldú, J. M. & Porter, M. A. Frequency-based brain networks: From a multiplex framework to a full multilayer description. *Network Neuroscience* **2**, 418–441 (2018). URL <https://www.ncbi.nlm.nih.gov/pmc/articles/PMC6147638/>.

- [32] Guillon, J. *et al.* Disrupted core-periphery structure of multimodal brain networks in Alzheimer’s disease. *Network Neuroscience* **3**, 635–652 (2019). URL http://dx.doi.org/10.1162/netn_a_00087. Publisher: MIT Press.
- [33] Cuffin, B. N. & Cohen, D. Comparison of the magnetoencephalogram and electroencephalogram. *Electroencephalography and Clinical Neurophysiology* **47**, 132–146 (1979).
- [34] Geisler, C. D. & Gerstein, G. L. The surface EEG in relation to its sources. *Electroencephalography and Clinical Neurophysiology* **13**, 927–934 (1961). URL [http://dx.doi.org/10.1016/0013-4694\(61\)90199-7](http://dx.doi.org/10.1016/0013-4694(61)90199-7).
- [35] Delucchi, M. R., Garoutte, B. & Aird, R. B. The scalp as an electroencephalographic averager. *Electroencephalography and Clinical Neurophysiology* **14**, 191–196 (1962).
- [36] Hämäläinen, M., Hari, R., Ilmoniemi, R. J., Knuutila, J. & Lounasmaa, O. V. Magnetoencephalography-theory, instrumentation, and applications to noninvasive studies of the working human brain. *Reviews of Modern Physics* **65**, 413–497 (1993). URL <http://dx.doi.org/10.1103/RevModPhys.65.413>.
- [37] Wood, C. C., Cohen, D., Cuffin, B. N., Yarita, M. & Allison, T. Electrical sources in human somatosensory cortex: identification by combined magnetic and potential recordings. *Science (New York, N.Y.)* **227**, 1051–1053 (1985). URL <https://science.sciencemag.org/content/227/4690/1051.long>.
- [38] Sharon, D., Hämäläinen, M. S., Tootell, R. B. H., Halgren, E. & Belliveau, J. W. The advantage of combining MEG and EEG: Comparison to fMRI in focally stimulated visual cortex. *Neuroimage* **36**, 1225–1235 (2007). URL <http://dx.doi.org/10.1016/j.neuroimage.2007.03.066>.
- [39] Corsi, M.-C. *et al.* Integrating EEG and MEG Signals to Improve Motor Imagery Classification in Brain–Computer Interface. *International Journal of Neural Systems* **29**, 1850014 (2018). URL <https://www.worldscientific.com/doi/abs/10.1142/S0129065718500144>.
- [40] Wolpaw, J. R., McFarland, D. J., Vaughan, T. M. & Schalk, G. The Wadsworth Center brain-computer interface (BCI) research and development program. *IEEE Transactions on Neural Systems and Rehabilitation Engineering* **11**, 204–207 (2003). URL <http://dx.doi.org/10.1109/TNSRE.2003.814442>.

- [41] Schalk, G., McFarland, D. J., Hinterberger, T., Birbaumer, N. & Wolpaw, J. R. BCI2000: a general-purpose brain-computer interface (BCI) system. *IEEE Transactions on Biomedical Engineering* **51**, 1034–1043 (2004). URL <http://dx.doi.org/10.1109/TBME.2004.827072>.
- [42] Oostenveld, R., Fries, P., Maris, E., Schoffelen, J.-M. & Oostenveld. FieldTrip: Open Source Software for Advanced Analysis of MEG, EEG, and Invasive Electrophysiological Data. *Computational Intelligence and Neuroscience* **2011**, e156869 (2010). URL <http://www.hindawi.com/journals/cin/2011/156869/abs/>.
- [43] Gross, J. *et al.* Good practice for conducting and reporting MEG research. *Neuroimage* **65**, 349–363 (2013). URL <http://dx.doi.org/10.1016/j.neuroimage.2012.10.001>.
- [44] Fischl, B. FreeSurfer. *Neuroimage* **62**, 774–781 (2012). URL <http://www.sciencedirect.com/science/article/pii/S1053811912000389>.
- [45] Tadel, F., Baillet, S., Mosher, J. C., Pantazis, D. & Leahy, R. M. Brainstorm: A User-Friendly Application for MEG/EEG Analysis. *Computational Intelligence and Neuroscience* **2011** (2011). URL <http://dx.doi.org/10.1155/2011/879716>.
- [46] Corsi, M.-C. *et al.* Functional disconnection of associative cortical areas predicts performance during BCI training. *Neuroimage* **209**, 116500 (2020). URL <http://www.sciencedirect.com/science/article/pii/S1053811919310912>.
- [47] Taulu, S. & Simola, J. Spatiotemporal signal space separation method for rejecting nearby interference in MEG measurements. *Physics in Medicine & Biology* **51**, 1759–1768 (2006). URL <http://dx.doi.org/10.1088/0031-9155/51/7/008>.
- [48] Bell, A. J. & Sejnowski, T. J. An information-maximization approach to blind separation and blind deconvolution. *Neural Computation* **7**, 1129–1159 (1995).
- [49] Fuchs, M., Wagner, M. & Kastner, J. Boundary element method volume conductor models for EEG source reconstruction. *Clinical Neurophysiology* **112**, 1400–1407 (2001). URL <http://www.sciencedirect.com/science/article/pii/S1388245701005892>.
- [50] Gramfort, A., Papadopoulos, T., Olivi, E. & Clerc, M. OpenMEEG: opensource software for quasistatic bioelectromagnetics. *BioMedical Engineering OnLine* **9**, 45 (2010). URL <http://dx.doi.org/10.1186/1475-925X-9-45>.

- [51] Fuchs, M., Wagner, M., Köhler, T. & Wischmann, H.-A. Linear and nonlinear current density reconstructions. *Journal of Clinical Neurophysiology* **16**, 267–295 (1999).
- [52] Lin, F.-H. *et al.* Assessing and improving the spatial accuracy in MEG source localization by depth-weighted minimum-norm estimates. *Neuroimage* **31**, 160–171 (2006). URL <http://dx.doi.org/10.1016/j.neuroimage.2005.11.054>.
- [53] Gramfort, A. *et al.* MNE software for processing MEG and EEG data. *Neuroimage* **86**, 446–460 (2014). URL <http://dx.doi.org/10.1016/j.neuroimage.2013.10.027>.
- [54] Destrieux, C., Fischl, B., Dale, A. & Halgren, E. Automatic parcellation of human cortical gyri and sulci using standard anatomical nomenclature. *Neuroimage* **53**, 1–15 (2010). URL <https://www.ncbi.nlm.nih.gov/pmc/articles/PMC2937159/>.
- [55] Sekihara, K., Owen, J., Trisno, S. & Nagarajan, S. S. Removal of spurious coherence in MEG source-space coherence analysis. *IEEE transactions on bio-medical engineering* **58**, 3121–3129 (2011). URL <https://www.ncbi.nlm.nih.gov/pmc/articles/PMC4096348/>.
- [56] Kennedy, J. & Eberhart, R. Particle swarm optimization. In *Proceedings of ICNN'95 - International Conference on Neural Networks*, vol. 4, 1942–1948 vol.4 (1995). URL <http://dx.doi.org/10.1109/ICNN.1995.488968>. ISSN: null.
- [57] Rubinov, M. & Sporns, O. Complex network measures of brain connectivity: Uses and interpretations. *Neuroimage* **52**, 1059–1069 (2010). URL <http://www.sciencedirect.com/science/article/pii/S105381190901074X>.
- [58] Klimesch, W. EEG alpha and theta oscillations reflect cognitive and memory performance: a review and analysis. *Brain Research Reviews* **29**, 169–195 (1999). URL <http://www.sciencedirect.com/science/article/pii/S0165017398000563>.
- [59] Pichiorri, F. *et al.* Brain-computer interface boosts motor imagery practice during stroke recovery. *Annals of Neurology* **77**, 851–865 (2015). URL <http://dx.doi.org/10.1002/ana.24390>.
- [60] Shapiro, S. S. & Wilk, M. B. An analysis of variance test for normality (complete samples). *Biometrika* **52**, 591–611 (1965). URL <https://academic.oup.com/biomet/article/52/3-4/591/336553>. Publisher: Oxford Academic.

- [61] Bakdash, J. Z. & Marusich, L. R. Repeated Measures Correlation. *Frontiers in Psychology* **8** (2017). URL <https://www.frontiersin.org/articles/10.3389/fpsyg.2017.00456/full>.
- [62] Benjamini, Y. & Yekutieli, D. The Control of the False Discovery Rate in Multiple Testing under Dependency. *The Annals of Statistics* **29**, 1165–1188 (2001). URL <https://www.jstor.org/stable/2674075>.
- [63] McAuley, E. Z. *et al.* Association between the serotonin 2a receptor gene and bipolar affective disorder in an Australian cohort. *Psychiatric Genetics* **19**, 244–252 (2009).
- [64] Sanders, M. S., van Well, G. T., Ouburg, S., Morré, S. A. & van Furth, A. M. Toll-like receptor 9 polymorphisms are associated with severity variables in a cohort of meningococcal meningitis survivors. *BMC Infectious Diseases* **12**, 112 (2012). URL <https://doi.org/10.1186/1471-2334-12-112>.
- [65] Matthews, D. E. & Farewell, V. T. *Using and Understanding Medical Statistics* (Karger Medical and Scientific Publishers, 2015). Google-Books-ID: DL8nCgAAQBAJ.
- [66] Müller-putz, G. R., Scherer, R., Brunner, C., Leeb, R. & Pfurtscheller, G. Better than random: a closer look on BCI results. *International Journal of Bioelectromagnetism* **10** (2008). URL <http://citeseerx.ist.psu.edu/viewdoc/download?doi=10.1.1.330.3349&rep=rep1&type=pdf>.
- [67] Aminoff, E. M., Kveraga, K. & Bar, M. The role of the parahippocampal cortex in cognition. *Trends in Cognitive Sciences* **17**, 379–390 (2013). URL <https://www.ncbi.nlm.nih.gov/pmc/articles/PMC3786097/>.
- [68] Kolling, N., Behrens, T. E., Wittmann, M. K. & Rushworth, M. F. Multiple signals in anterior cingulate cortex. *Current Opinion in Neurobiology* **37**, 36–43 (2016). URL <http://www.sciencedirect.com/science/article/pii/S0959438815001853>.
- [69] Uddin, L. Q., Nomi, J. S., Hebert-Seropian, B., Ghaziri, J. & Boucher, O. Structure and function of the human insula. *Journal of Clinical Neurophysiology* **34**, 300–306 (2017). URL <https://www.ncbi.nlm.nih.gov/pmc/articles/PMC6032992/>.
- [70] Du, J. *et al.* Functional connectivity of the orbitofrontal cortex, anterior cingulate cortex, and inferior frontal gyrus in humans. *Cortex* **123**, 185–199 (2020). URL <http://www.sciencedirect.com/science/article/pii/S001094521930365X>.

- [71] Bonnefond, M. *et al.* What MEG can reveal about inference making: The case of if...then sentences. *Human Brain Mapping* **34**, 684–697 (2012). URL <https://www.ncbi.nlm.nih.gov/pmc/articles/PMC6870271/>.
- [72] Nee, D. E. *et al.* A Meta-analysis of Executive Components of Working Memory. *Cerebral Cortex* **23**, 264–282 (2013). URL <https://academic.oup.com/cercor/article/23/2/264/283011>. Publisher: Oxford Academic.
- [73] Milivojevic, B., Hamm, J. P. & Corballis, M. C. Functional neuroanatomy of mental rotation. *Journal of Cognitive Neuroscience* **21**, 945–959 (2009). URL <http://dx.doi.org/10.1162/jocn.2009.21085>.
- [74] Wilson, R. C., Takahashi, Y. K., Schoenbaum, G. & Niv, Y. Orbitofrontal Cortex as a Cognitive Map of Task Space. *Neuron* **81**, 267–279 (2014). URL <http://www.sciencedirect.com/science/article/pii/S0896627313010398>.
- [75] Christophel, T. B., Klink, P. C., Spitzer, B., Roelfsema, P. R. & Haynes, J.-D. The Distributed Nature of Working Memory. *Trends in Cognitive Sciences* **21**, 111–124 (2017). URL <http://www.sciencedirect.com/science/article/pii/S1364661316302170>.
- [76] Euston, D. R., Gruber, A. J. & McNaughton, B. L. The Role of Medial Prefrontal Cortex in Memory and Decision Making. *Neuron* **76**, 1057–1070 (2012). URL [https://www.cell.com/neuron/abstract/S0896-6273\(12\)01108-7](https://www.cell.com/neuron/abstract/S0896-6273(12)01108-7).
- [77] Stephan, K. M. *et al.* Functional anatomy of the mental representation of upper extremity movements in healthy subjects. *Journal of Neurophysiology* **73**, 373–386 (1995). URL <http://dx.doi.org/10.1152/jn.1995.73.1.373>.
- [78] Johnson, S. H. *et al.* Selective activation of a parietofrontal circuit during implicitly imagined prehension. *Neuroimage* **17**, 1693–1704 (2002). URL <https://www.sciencedirect.com/science/article/abs/pii/S1053811902912656?via%3Dihub>.
- [79] Solodkin, A., Hlustik, P., Chen, E. E. & Small, S. L. Fine modulation in network activation during motor execution and motor imagery. *Cerebral Cortex* **14**, 1246–1255 (2004). URL <http://dx.doi.org/10.1093/cercor/bhh086>.
- [80] Rizzolatti, G. *et al.* Localization of grasp representations in humans by PET: 1. Observation versus execution. *Experimental Brain Research* **111**, 246–252 (1996). URL <https://doi.org/10.1007>

BF00227301.

- [81] Silver, M. A., Ress, D. & Heeger, D. J. Neural correlates of sustained spatial attention in human early visual cortex. *Journal of Neurophysiology* **97**, 229–237 (2007). URL <http://dx.doi.org/10.1152/jn.00677.2006>.
- [82] Yousry, T. A. *et al.* Localization of the motor hand area to a knob on the precentral gyrus. A new landmark. *Brain* **120**, 141–157 (1997). URL <https://academic.oup.com/brain/article/120/1/141/312820>.
- [83] Lotze, M. & Halsband, U. Motor imagery. *Journal of Physiology-Paris* **99**, 386–395 (2006). URL <http://www.sciencedirect.com/science/article/pii/S0928425706000210>.
- [84] van de Nieuwenhuijzen, M. E. *et al.* MEG-based decoding of the spatiotemporal dynamics of visual category perception. *Neuroimage* **83**, 1063–1073 (2013). URL <https://www.sciencedirect.com/science/article/abs/pii/S1053811913008446?via%3Dihub>.
- [85] Allison, B. Z. & Neuper, C. Could Anyone Use a BCI? In Tan, D. S. & Nijholt, A. (eds.) *Brain-Computer Interfaces*, Human-Computer Interaction Series, 35–54 (Springer London, 2010). URL http://link.springer.com/chapter/10.1007/978-1-84996-272-8_3.
- [86] Ganguly, K. & Carmena, J. M. Emergence of a stable cortical map for neuroprosthetic control. *PLoS Biology* **7**, e1000153 (2009). URL <http://journals.plos.org/plosbiology/article?id=10.1371/journal.pbio.1000153>.
- [87] Carmena, J. M. *et al.* Learning to control a brain-machine interface for reaching and grasping by primates. *PLoS Biology* **1**, E42 (2003). URL <http://journals.plos.org/plosbiology/article?id=10.1371/journal.pbio.0000042>.
- [88] Perdakis, S. & Millan, J. d. R. Brain-Machine Interfaces: A Tale of Two Learners. *IEEE Systems, Man, and Cybernetics Magazine* **6**, 12–19 (2020). URL <https://ieeexplore.ieee.org/document/9141465>.
IEEE Systems, Man, and Cybernetics Magazine.
- [89] Dayan, P. & Niv, Y. Reinforcement learning: the good, the bad and the ugly. *Current Opinion in Neurobiology* **18**, 185–196 (2008). URL <http://dx.doi.org/10.1016/j.conb.2008.08.003>.

- [90] Stiso, J. *et al.* Learning in brain-computer interface control evidenced by joint decomposition of brain and behavior. *Journal of Neural Engineering* (2020). URL <http://dx.doi.org/10.1088/1741-2552/ab9064>.
- [91] van den Heuvel, M. P. & Sporns, O. Network hubs in the human brain. *Trends in Cognitive Sciences* **17**, 683–696 (2013). URL <http://dx.doi.org/10.1016/j.tics.2013.09.012>.
- [92] van den Heuvel, M. P. & Hulshoff Pol, H. E. Exploring the brain network: A review on resting-state fMRI functional connectivity. *European Neuropsychopharmacology* **20**, 519–534 (2010). URL <http://www.sciencedirect.com/science/article/pii/S0924977X10000684>.
- [93] van den Heuvel, M. P. *et al.* Abnormal rich club organization and functional brain dynamics in schizophrenia. *JAMA Psychiatry* **70**, 783–792 (2013). URL <http://dx.doi.org/10.1001/jamapsychiatry.2013.1328>.
- [94] Klimesch, W., Sauseng, P. & Hanslmayr, S. EEG alpha oscillations: the inhibition-timing hypothesis. *Brain Res Rev* **53**, 63–88 (2007). URL <https://www.sciencedirect.com/science/article/abs/pii/S016501730600083X?via%3Dihub>.
- [95] Jensen, O. & Mazaheri, A. Shaping Functional Architecture by Oscillatory Alpha Activity: Gating by Inhibition. *Frontiers in Human Neuroscience* **4** (2010). URL <https://www.frontiersin.org/articles/10.3389/fnhum.2010.00186/full#B28>. Publisher: Frontiers.
- [96] Haegens, S., Nacher, V., Luna, R., Romo, R. & Jensen, O. α -Oscillations in the monkey sensorimotor network influence discrimination performance by rhythmical inhibition of neuronal spiking. *Proceedings of the National Academy of Sciences of the United States of America* **108**, 19377–19382 (2011). URL <https://www.pnas.org/content/early/2011/11/09/1117190108>.
- [97] Spitzer, B. & Haegens, S. Beyond the Status Quo: A Role for Beta Oscillations in Endogenous Content (Re)Activation. *eNeuro* **4** (2017). URL <https://www.ncbi.nlm.nih.gov/pmc/articles/PMC5539431/>.
- [98] Engel, A. K. & Fries, P. Beta-band oscillations—signalling the status quo? *Current Opinion in Neurobiology* **20**, 156–165 (2010). URL <https://www.sciencedirect.com/science/article/abs/pii/S0959438810000395?via%3Dihub>.

- [99] Donner, T. H. *et al.* Population activity in the human dorsal pathway predicts the accuracy of visual motion detection. *Journal of Neurophysiology* **98**, 345–359 (2007). URL <https://journals.physiology.org/doi/full/10.1152/jn.01141.2006>.
- [100] Piantoni, G., Kline, K. A. & Eagleman, D. M. Beta oscillations correlate with the probability of perceiving rivalrous visual stimuli. *Journal of Vision* **10**, 18 (2010). URL <https://jov.arvojournals.org/article.aspx?articleid=2191657>.
- [101] Siegel, M., Warden, M. R. & Miller, E. K. Phase-dependent neuronal coding of objects in short-term memory. *Proceedings of the National Academy of Sciences of the United States of America* **106**, 21341–21346 (2009). URL <https://www.pnas.org/content/106/50/21341>.
- [102] Muthuraman, M. *et al.* Beamformer source analysis and connectivity on concurrent EEG and MEG data during voluntary movements. *PloS One* **9** (2014). URL <http://dx.doi.org/10.1371/journal.pone.0091441>.
- [103] Coquelet, N. *et al.* Comparing MEG and high-density EEG for intrinsic functional connectivity mapping. *Neuroimage* 116556 (2020). URL <http://www.sciencedirect.com/science/article/pii/S1053811920300434>.
- [104] Perdakis, S., Leeb, R. & Millán, J. d. R. Subject-oriented training for motor imagery brain-computer interfaces. *Conference Proceedings IEEE Engineering in Medicine and Biology Society* **2014**, 1259–1262 (2014). URL <http://dx.doi.org/10.1109/EMBC.2014.6943826>.
- [105] De Vico Fallani, F. & Bassett, D. S. Network neuroscience for optimizing brain-computer interfaces. *Physics of Life Reviews* (2019). URL <http://www.sciencedirect.com/science/article/pii/S1571064519300016>.
- [106] Benaroch, C., Jeunet, C. & Lotte, F. Are users’ traits informative enough to predict/explain their mental-imagery based BCI performances? In *GBCIC 2019*, 7 (2019).
- [107] Ahn, M., Cho, H., Ahn, S. & Jun, S. C. High theta and low alpha powers may be indicative of BCI-illiteracy in motor imagery. *PLoS ONE* **8**, e80886 (2013). URL <http://dx.doi.org/10.1371/journal.pone.0080886>.
- [108] Jeunet, C., N’Kaoua, B., Subramanian, S., Hachet, M. & Lotte, F. Predicting Mental Imagery-Based BCI Performance from Personality, Cognitive Profile and Neurophysiological Patterns. *PLoS ONE* **10**,

- e0143962 (2015). URL <http://dx.doi.org/10.1371/journal.pone.0143962>.
- [109] Sugata, H. *et al.* Alpha band functional connectivity correlates with the performance of brain-machine interfaces to decode real and imagined movements. *Frontiers in Human Neuroscience* **8** (2014). URL <https://doi.org/10.3389%2Ffnhum.2014.00620>.
- [110] De Vico Fallani, F. *et al.* Multiscale topological properties of functional brain networks during motor imagery after stroke. *Neuroimage* **83**, 438–449 (2013). URL <http://dx.doi.org/10.1016/j.neuroimage.2013.06.039>.
- [111] Li, J. *et al.* Probabilistic diffusion tractography reveals improvement of structural network in musicians. *PLoS ONE* **9**, e105508 (2014). URL <https://journals.plos.org/plosone/article?id=10.1371/journal.pone.0105508>.
- [112] Calmels, C. Neural correlates of motor expertise: Extensive motor training and cortical changes. *Brain Research* **1739**, 146323 (2020). URL <http://www.sciencedirect.com/science/article/pii/S0006899319303695>.
- [113] Héту, S. *et al.* The neural network of motor imagery: an ALE meta-analysis. *Neuroscience & Biobehavioral Reviews* **37**, 930–949 (2013). URL <http://dx.doi.org/10.1016/j.neubiorev.2013.03.017>.
- [114] Hardwick, R. M., Caspers, S., Eickhoff, S. B. & Swinnen, S. P. Neural correlates of action: Comparing meta-analyses of imagery, observation, and execution. *Neuroscience & Biobehavioral Reviews* **94**, 31–44 (2018). URL <http://www.sciencedirect.com/science/article/pii/S0149763417309284>.
- [115] Dayan, E. & Cohen, L. G. Neuroplasticity subserving motor skill learning. *Neuron* **72**, 443–454 (2011). URL <https://www.ncbi.nlm.nih.gov/pmc/articles/PMC3217208/>.
- [116] van Zomeren, A. H. & Brouwer, W. H. *Clinical neuropsychology of attention*. Clinical neuropsychology of attention (Oxford University Press, New York, NY, US, 1994).
- [117] Wolpert, D. M. & Landy, M. S. Motor Control is Decision-Making. *Current Opinion in Neurobiology* **22**, 996–1003 (2012). URL <https://www.ncbi.nlm.nih.gov/pmc/articles/PMC3434279/>.
- [118] Guillot, A. & Collet, C. (eds.) *The neurophysiological foundations of mental and motor imagery* (Oxford University Press, Oxford, New York, 2010).
- [119] Wulf, G. *Attention and motor skill learning*. Attention and motor skill learning (Human Kinetics, Champaign, IL, US, 2007).

- [120] Lohse, K. R., Jones, M., Healy, A. F. & Sherwood, D. E. The role of attention in motor control. *Journal of Experimental Psychology: General* **143**, 930–948 (2014). URL <http://dx.doi.org/10.1037/a0032817>.
- [121] Dayan, P., Kakade, S. & Montague, P. R. Learning and selective attention. *Nature Neuroscience* **3**, 1218–1223 (2000). URL https://www.nature.com/articles/nn1100_1218.
- [122] Gottlieb, J. Attention, Learning, and the Value of Information. *Neuron* **76**, 281–295 (2012). URL <http://www.sciencedirect.com/science/article/pii/S0896627312008884>.
- [123] Yin, H. H. *et al.* Dynamic reorganization of striatal circuits during the acquisition and consolidation of a skill. *Nature Neuroscience* **12**, 333–341 (2009). URL <https://www.ncbi.nlm.nih.gov/pmc/articles/PMC2774785/>.
- [124] Boto, E. *et al.* A new generation of magnetoencephalography: Room temperature measurements using optically-pumped magnetometers. *NeuroImage* **149**, 404 – 414 (2017). URL <http://www.sciencedirect.com/science/article/pii/S1053811917300411>.
- [125] Labyt, E. *et al.* Magnetoencephalography with optically pumped ⁴He magnetometers at ambient temperature. *IEEE Transactions on Medical Imaging* (2018). URL <https://ieeexplore.ieee.org/document/8411463>.
- [126] Boto, E. *et al.* Wearable neuroimaging: Combining and contrasting magnetoencephalography and electroencephalography. *Neuroimage* 116099 (2019). URL <http://www.sciencedirect.com/science/article/pii/S1053811919306901>.
- [127] Tierney, T. M. *et al.* Optically pumped magnetometers: From quantum origins to multi-channel magnetoencephalography. *Neuroimage* (2019). URL <http://www.sciencedirect.com/science/article/pii/S1053811919304550>.
- [128] Mitchell, S. M., Lange, S. & Brus, H. Gendered citation patterns in international relations journals. *International Studies Perspectives* **14**, 485–492 (2013).
- [129] Dion, M. L., Sumner, J. L. & Mitchell, S. M. Gendered citation patterns across political science and social science methodology fields. *Political Analysis* **26**, 312–327 (2018).
- [130] Caplar, N., Tacchella, S. & Birrer, S. Quantitative evaluation of gender bias in astronomical publications from citation counts. *Nature Astronomy* **1**, 0141 (2017).

- [131] Maliniak, D., Powers, R. & Walter, B. F. The gender citation gap in international relations. *International Organization* **67**, 889–922 (2013).
- [132] Dworkin, J. D. *et al.* The extent and drivers of gender imbalance in neuroscience reference lists. *bioRxiv* (2020). URL <https://www.biorxiv.org/content/early/2020/01/11/2020.01.03.894378>.
<https://www.biorxiv.org/content/early/2020/01/11/2020.01.03.894378.full.pdf>.
- [133] Zhou, D. *et al.* Gender diversity statement and code notebook v1.0 (2020). URL <https://doi.org/10.5281/zenodo.3672110>.
- [134] Ambekar, A., Ward, C., Mohammed, J., Male, S. & Skiena, S. Name-ethnicity classification from open sources. In *Proceedings of the 15th ACM SIGKDD international conference on Knowledge Discovery and Data Mining*, 49–58 (2009).
- [135] Sood, G. & Laohaprapanon, S. Predicting race and ethnicity from the sequence of characters in a name. *arXiv preprint arXiv:1805.02109* (2018).

Acknowledgments

This work was partially supported by French program "Investissements d'avenir" ANR-10-IAIHU-06; "ANR-NIH CRCNS" ANR-15-NEUC-0006-02 and by NICHD 1R01HD086888-01. The funders had no role in study design, data collection and analysis, decision to publish, or preparation of the manuscript. This work was performed on a platform of France Life Imaging network partly funded by the grant "ANR-11-INBS-0006".

Citation Diversity Statement

Recent work in several fields of science has identified a bias in citation practices such that papers from women and other minority scholars are under-cited relative to the number of such papers in the field [128, 129, 130, 131, 132]. Here we sought to proactively consider choosing references that reflect the diversity of the field in thought, form of contribution, gender, race, ethnicity, and other factors. We used automatic classification of gender based on the first names of the first and last authors [132, 133], with possible combinations including man/ man, man/woman, woman/man, and woman/woman. Code for this classification is open source and available online [133]. By this measure (and excluding self-citations to the first and last authors of our current paper), our references contain 4.96% woman(first)/woman(last), 13.24% man/woman, 16.34% woman/man, and 65.47% man/man. Second, we obtained predicted racial/ethnic category of the first and last author of

each reference by databases that store the probability of a first and last name being carried by an author of color [134, 135]. By this measure (and excluding self-citations), our references contain 12.99% author of color (first)/author of color(last), 14.83% white author/author of color, 21.91% author of color/white author, and 50.26% white author/white author. We look forward to future work that could help us to better understand how to support equitable practices in science.

Authors contributions

MC, DS, NG, LH, SD, DSB and FDVF initiated research; MCC, MC, DS, LH, DSB and FDVF designed research; MCC, DS and LH performed research; MCC, DS, LH and AEK contributed analytic tools; MCC and AEK analyzed data; and MCC, DSB, and FDVF wrote the paper. All authors revised and approved the manuscript.

Additional Information

Supplementary Information accompanies this paper.

BCI learning induces core-periphery reorganization in M/EEG multiplex brain networks

M.-C. Corsi* et al

March 18, 2021

Supplementary Figures

arXiv:2010.13459v2 [q-bio.NC] 17 Mar 2021

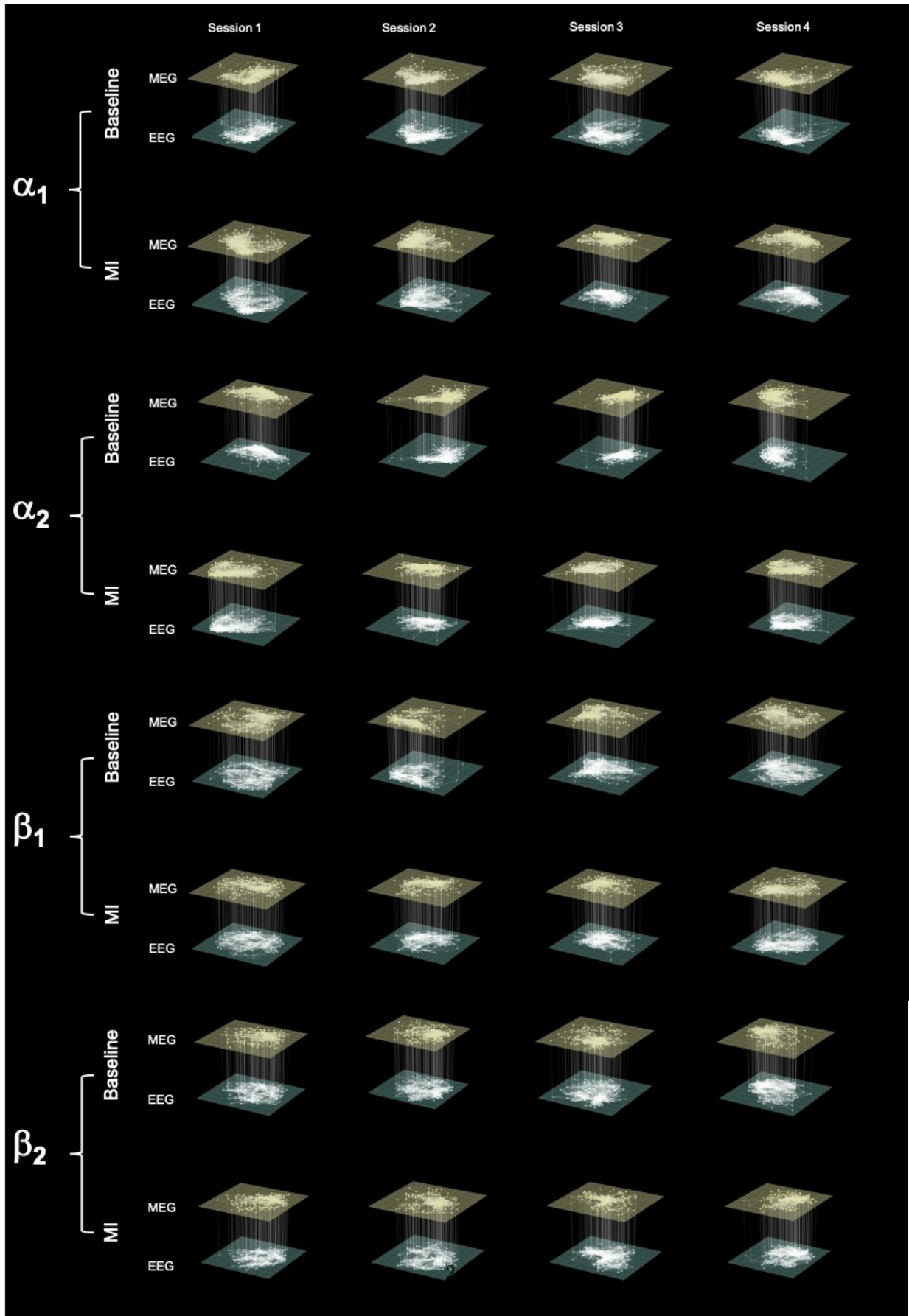


Figure S1: Evolution of the single layers for each condition within the α and the β ranges (average over the participants).

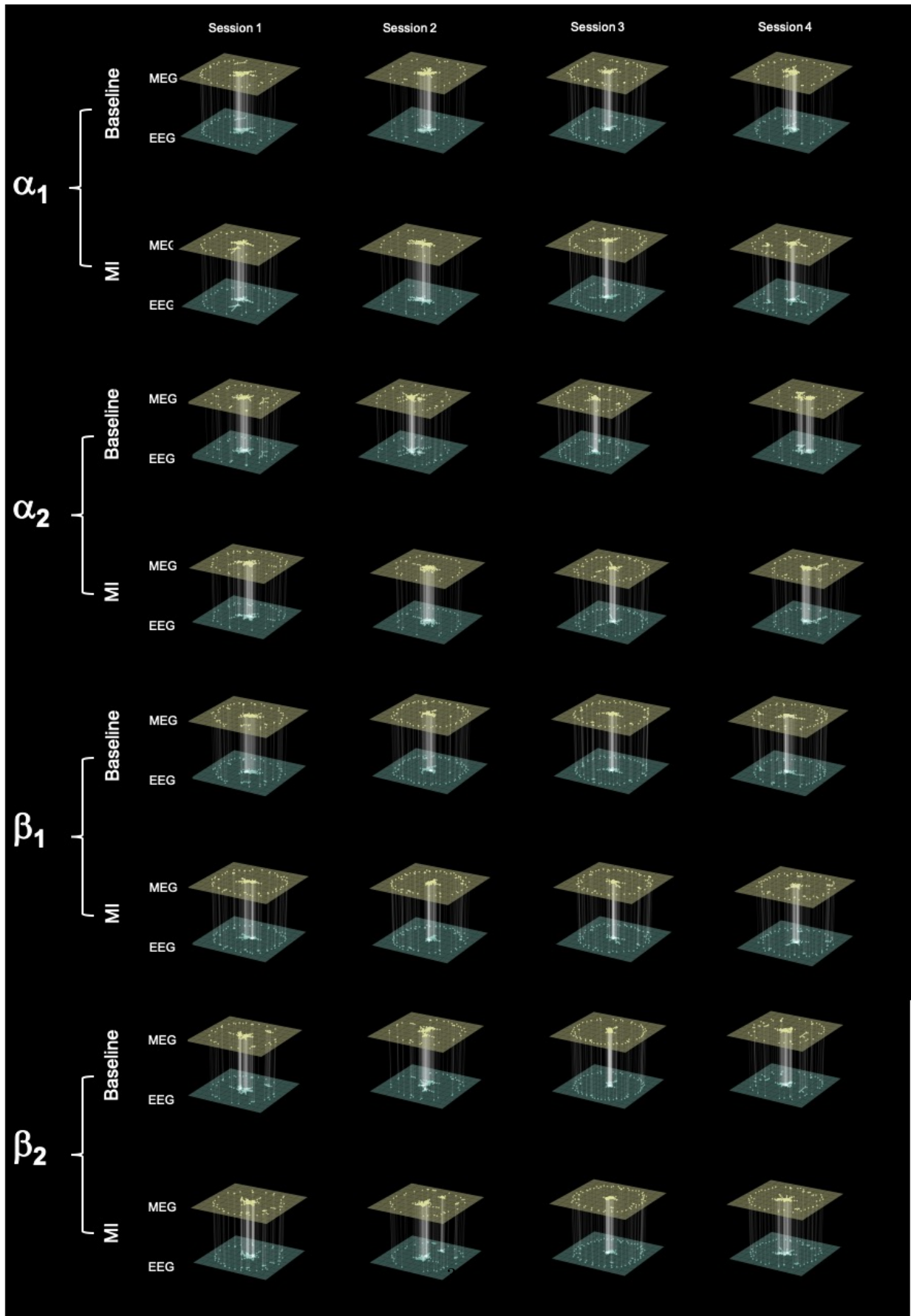
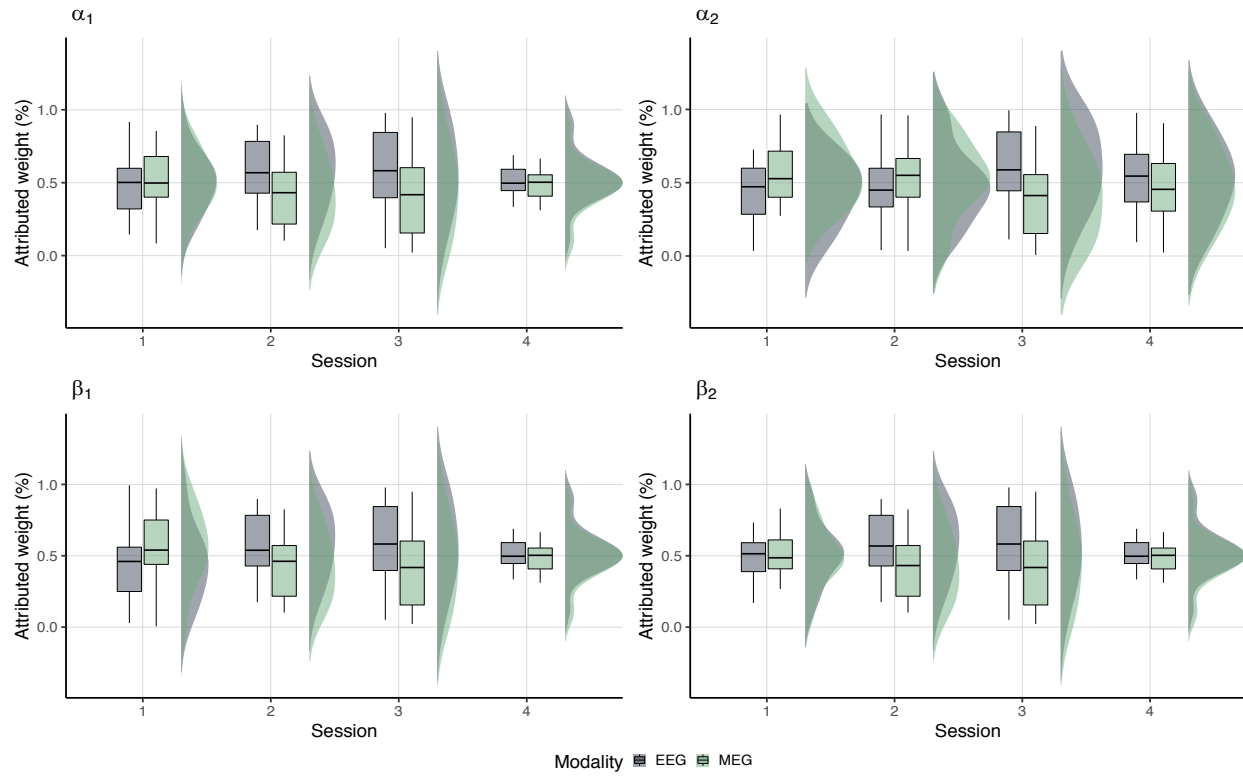


Figure S2: Evolution of the single layers for each condition within the α and the β ranges (Subject 03).



	Modality effect	Session effect	Interaction effect
α_1	F(1,152) = 5.15, p = 0.025	F(3,152) = 0.00, p = 1.000	F(3, 152) = 1.19, p = 0.315
α_2	F(1,152) = 0.31, p = 0.579	F(3,152) = 0.00, p = 1.000	F(3, 152) = 3.47, p = 0.018
β_1	F(1,152) = 1.90, p = 0.170	F(3, 152) = 0.00, p = 1.000	F(3, 152) = 2.84, p = 0.040
β_2	F(1,152) = 5.59, p = 0.019	F(3, 152) = 0.00, p = 1.000	F(3, 152) = 0.88, p = 0.456

Figure S3: Evolution of attributed weights over sessions within the α and the β ranges. We performed a two-way ANOVA using permutation tests.

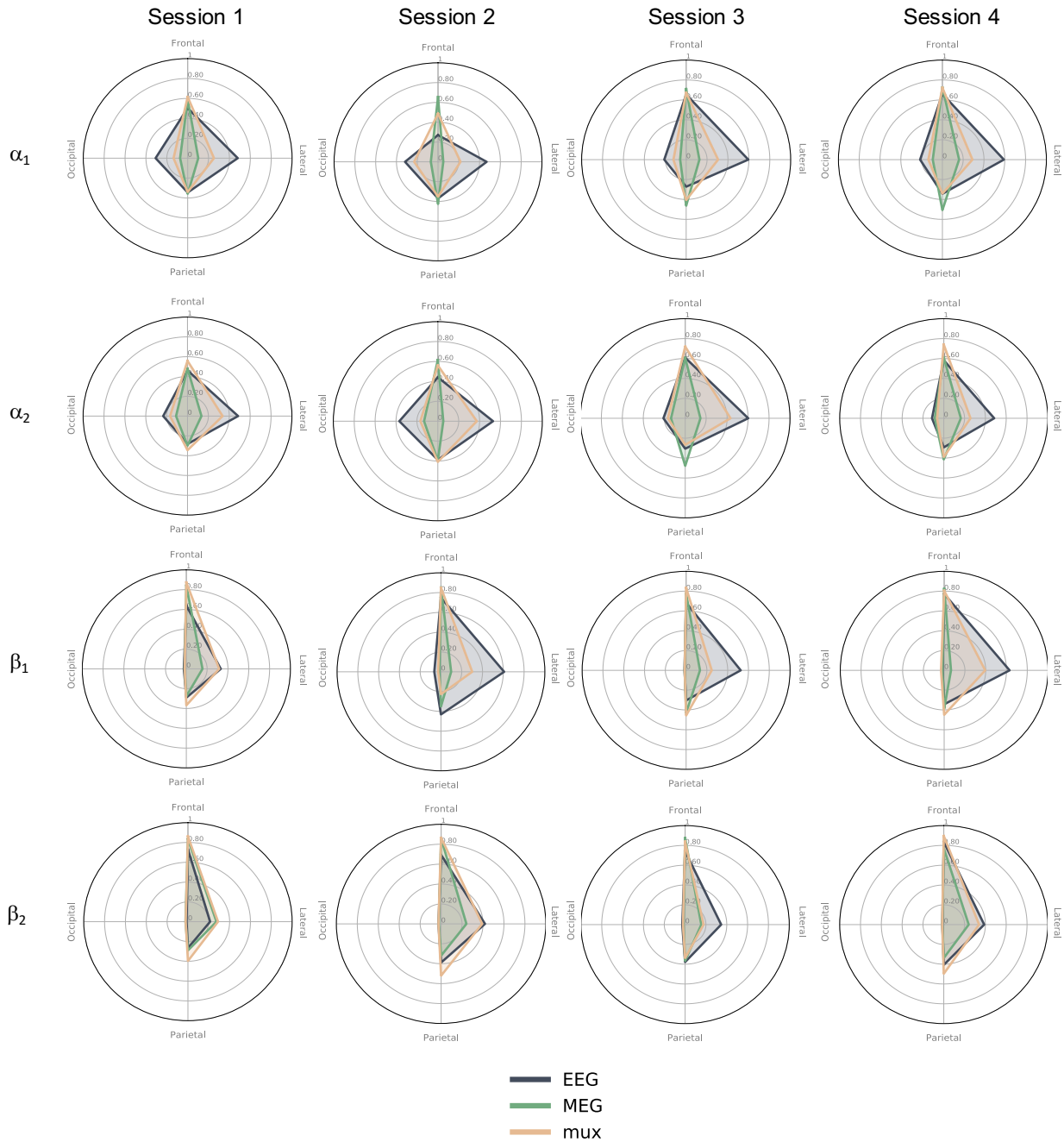


Figure S4: Evolution of single layer and multiplex coreness values over the BCI training in MI condition. For a given axis associated with a single brain lobe, we plotted the median coreness value obtained across the subjects and the ROIs that belong to the lobe, respectively in EEG, MEG and multiplex (mux). Each line corresponds to a specific frequency band (respectively α_1 , α_2 , β_1 and β_2) and each column to a specific session.

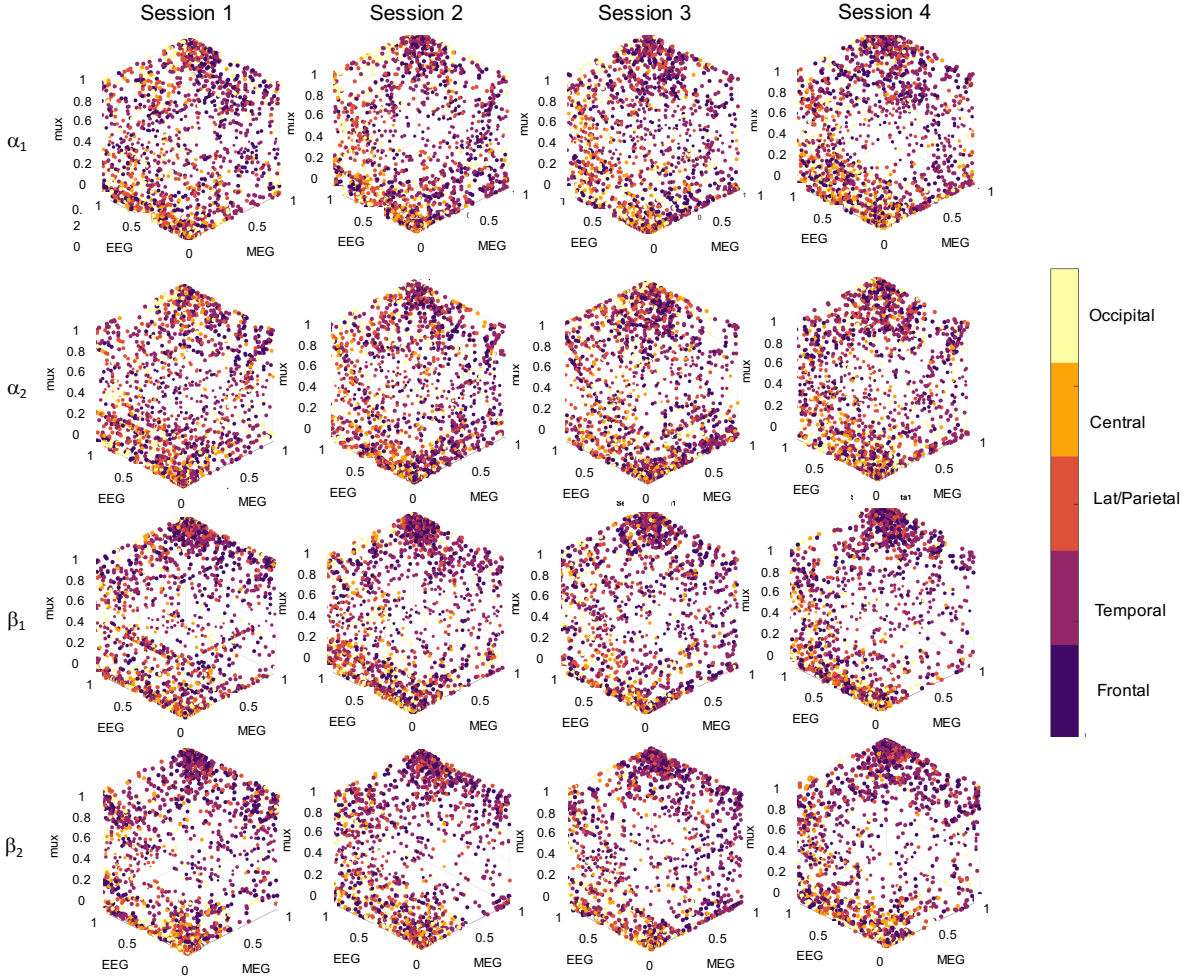


Figure S5: Evolution of single layer and multiplex coreness over the sessions in MI condition. For a given point associated with a single ROI and a single subject, its (x,y,z) coordinates correspond to the associated coreness value respectively in EEG, MEG, and multiplex (mux) and its color to its associated brain region. Each line corresponds to a specific frequency band and each column to a given session. We observed a cluster of ROIs (C11) that presents a maximal level of coreness in every modality in most of the sessions, both with α and β frequency ranges. They mostly belonged to frontal, lateral, and temporal lobes. More specifically, in the α_2 frequency band, we observed a homogeneous distribution of points at the beginning of training. Then, two main clusters appeared, C11 and another, mostly in the plane $C_{MEG} = 0$ (C12) involving ROIs located in central, latero-parietal, and temporal lobes. In the β_1 frequency band, we obtained a distribution less homogeneous than in α_2 with C11 and the appearance of two other clusters in the plane $C_{MEG} = 0$. One is associated with C_{Mux} larger than 0.3 (C13) gathering ROIs that belong to central, frontal, and temporal areas. The other (C14) is characterized by a minimal level of coreness in every modality associated with ROIs that mainly belong to occipital and central areas.

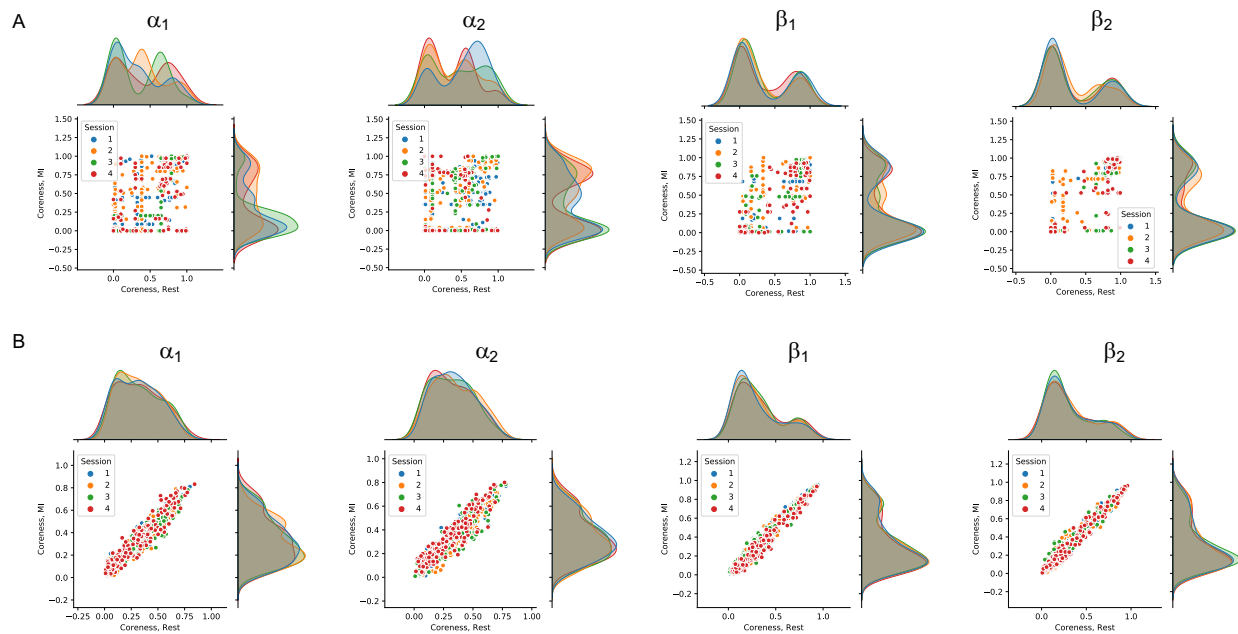
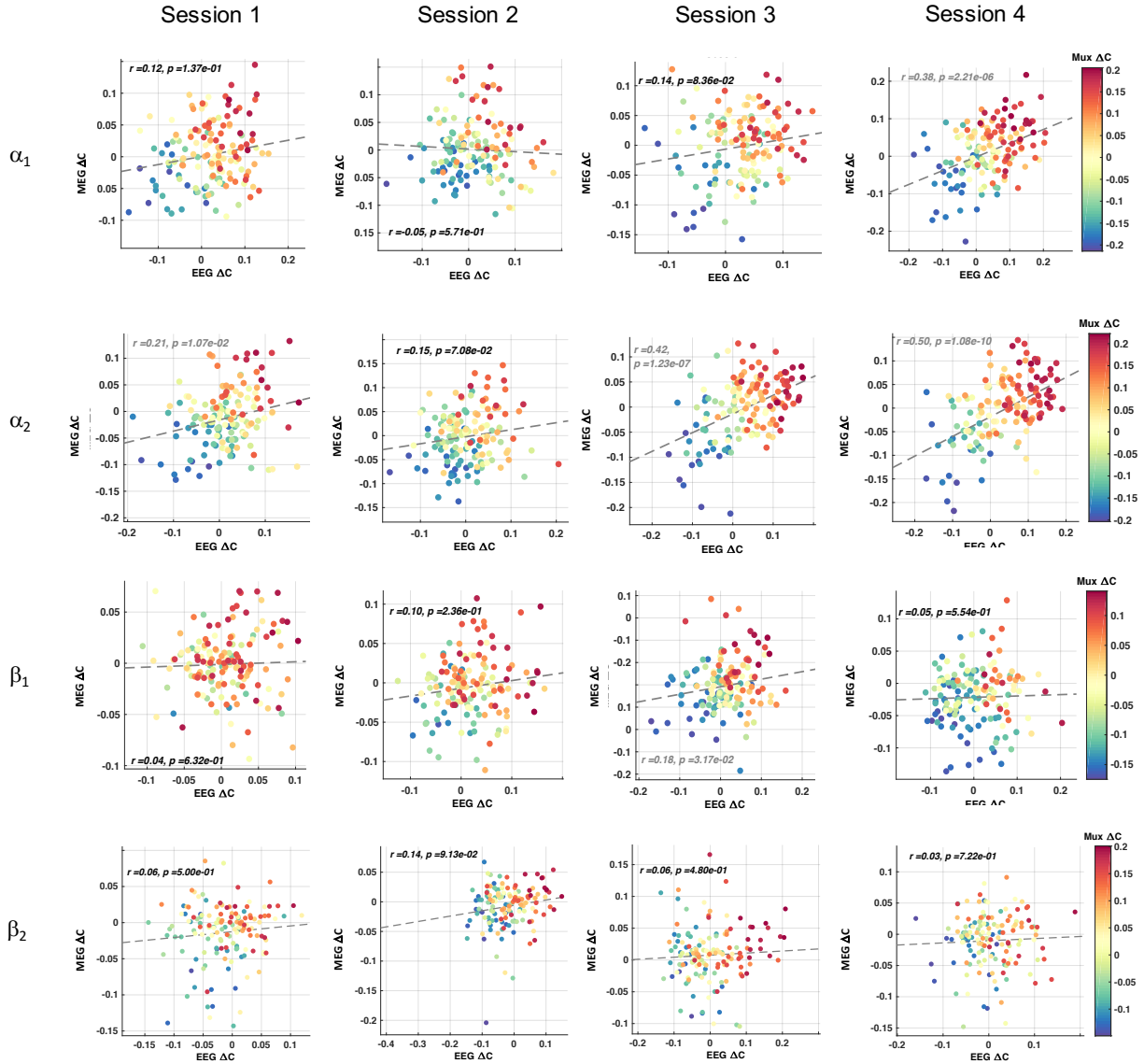


Figure S6: Multiplex coreness evolution over the training and the conditions, within the α and the β ranges. Each dot corresponds to a given ROI. On the X axis are represented the coreness values obtained during the Rest condition; on the Y axis are presented the coreness values obtained during the MI condition. (A) Results obtained from Subject 03. (B) Results obtained from the average performed over the subjects. The strong inter-subject variability engenders a lack of separability between conditions when one considers the average over the subjects.



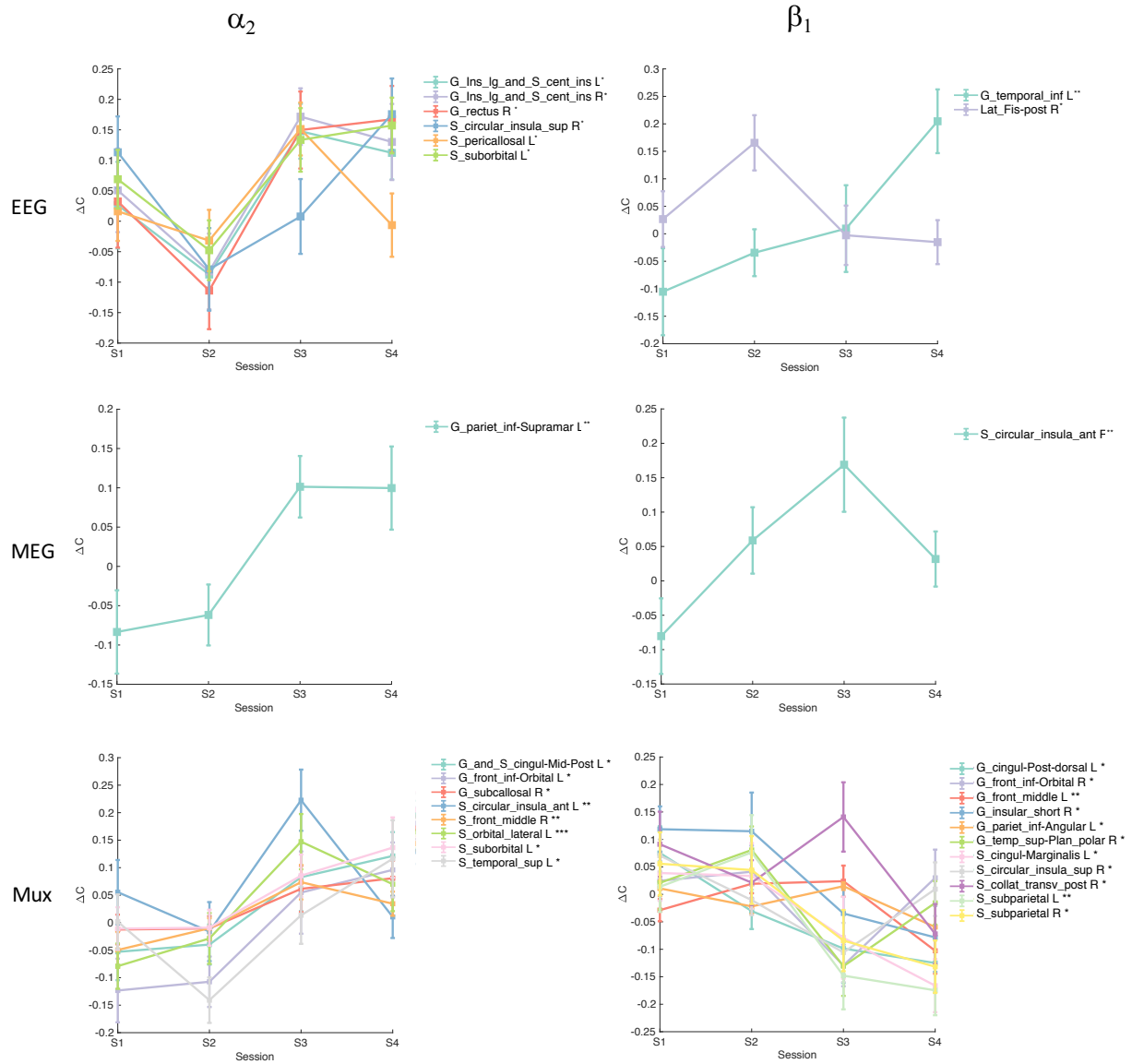


Figure S8: Distribution of relative coreness over the training in the α_2 and β_1 frequency bands. Only the ROIs that present a significant session effect are represented (one-way ANOVA, $p < 0.05$). Modalities were considered separately.

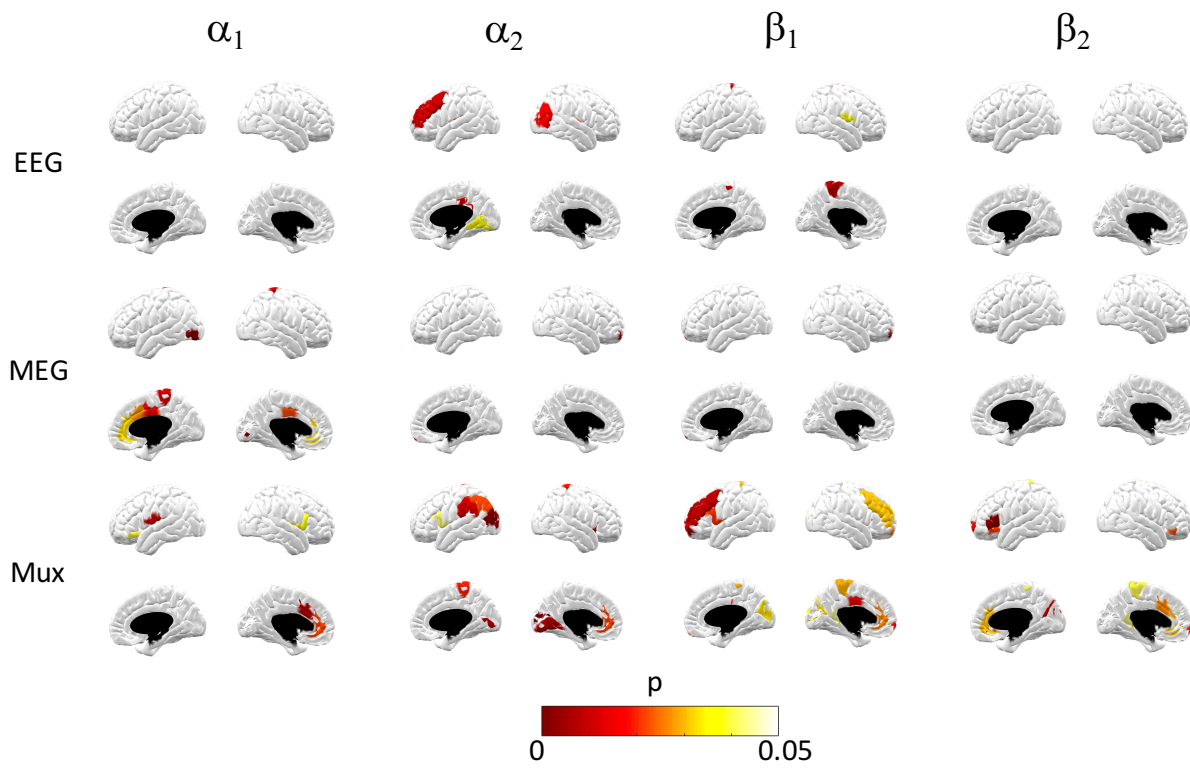


Figure S9: Significant session effect obtained with relative coreness (one-way ANOVA, $p < 0.05$) over sessions in the α and β frequency ranges. Modalities were considered separately.

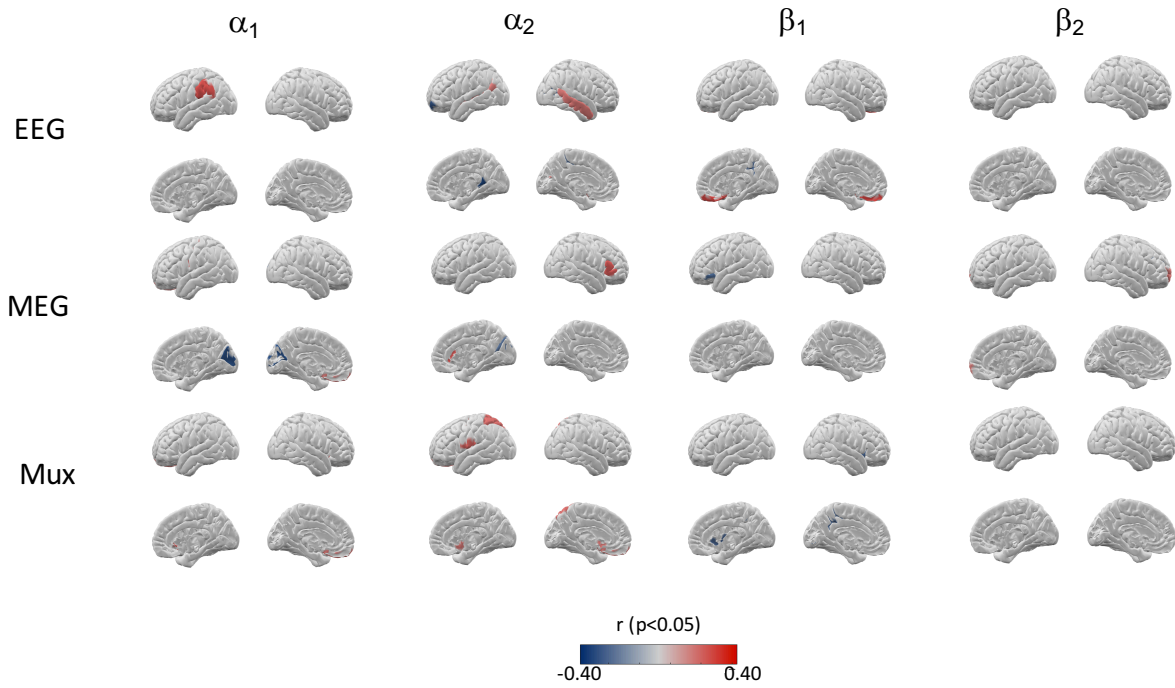


Figure S10: Repeated correlations between relative coreness and BCI scores in EEG, MEG, and mux ($p < 0.05$) within the α and the β frequency ranges.

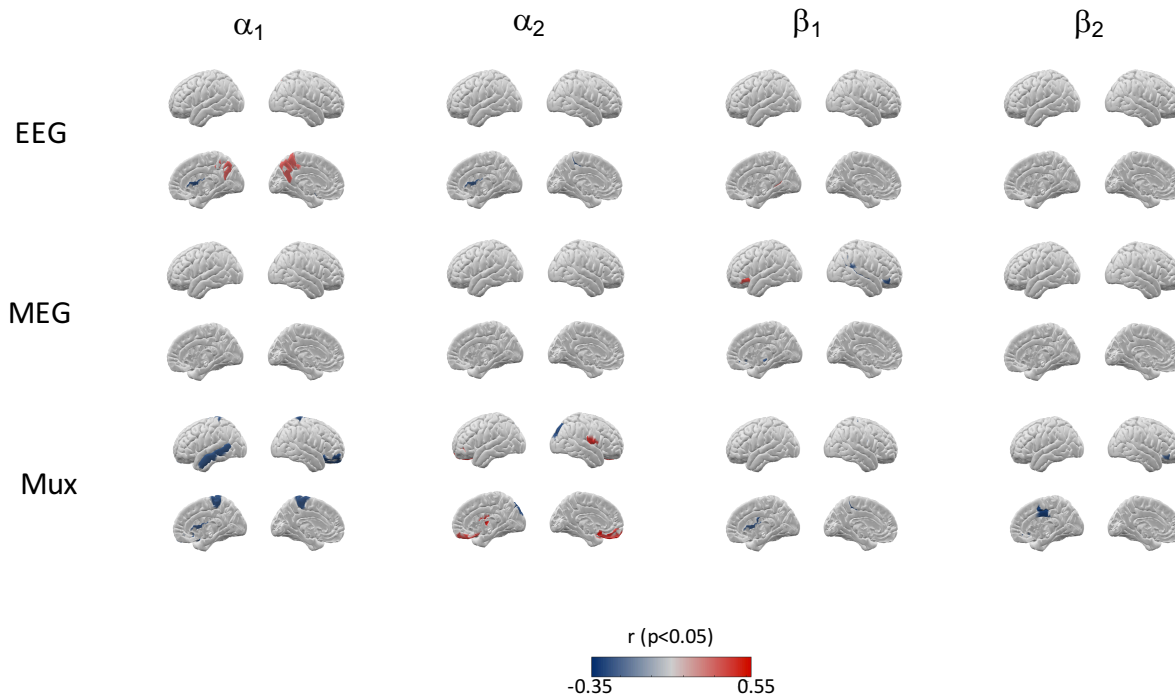


Figure S11: Repeated correlations between relative coreness and BCI scores obtained in the subsequent session in EEG, MEG, and mux ($p < 0.05$) within the α and the β frequency ranges.

Supplementary Tables

Table S1: List of ROIs that show a significant condition effect at least once during the training in the EEG modality ($p < 0.021$). In β_2 , we did not observe any significant result.

Frequency bands	ROI	(t, p)	Session
α_1	Anterior part of the cingulate gyrus and sulcus L	(3.02, 0.007)	S3
	Anterior part of the cingulate gyrus and sulcus R	(2.55, 0.020)	S4
	Middle-Anterior part of the cingulate gyrus and sulcus L	(2.92, 0.009)	S4
	Opercular part of the inferior frontal gyrus R	(2.81, 0.011)	S4
	Lateral occipito-temporal gyrus R	(2.73, 0.013)	S2
	Superior occipital gyrus L	(-2.54, 0.020)	S1
	Precuneus L	(-2.37, 0.028; -3.79, 0.001)	(S1; S2)
	Planum polare of the superior temporal gyrus L	(3.13, 0.005)	S4
	Vertical ramus of the anterior segment of the lateral sulcus R	(2.66, 0.016)	S4
	Long insular gyrus and central sulcus of the insula L	(3.28, 0.004; 2.57, 0.019)	(S3; S4)
	Long insular gyrus and central sulcus of the insula R	(3.69, 0.002)	S3
α_2	Middle-Anterior part of the cingulate gyrus and sulcus L	(2.72, 0.014)	S4
	Middle-posterior part of the cingulate gyrus and sulcusL	(2.81, 0.011)	S3
	Orbital part of the inferior frontal gyrus R	(2.58, 0.018)	S4
	Lingual gyrus R	(2.58, 0.018)	S4
	Superior parietal lobule L	(-3.46, 0.003)	S1
	Postcentral gyrus R	(-2.29, 0.034)	S2
	Gyrus rectus L	(2.61, 0.017)	S3
	Gyrus rectus R	(3.05, 0.007)	S4
	Posterior ramus (or segment) of the lateral sulcus (or fissure) R	(3.07, 0.006)	S1
	Temporal pole R	(3.18, 0.005)	S1
	Transverse frontopolar gyri and sulci R	(2.71, 0.014)	S2
β_1	Subcallosal gyrus R	(2.65, 0.016)	S3
	Anterior transverse temporal gyrus L	(2.60, 0.017)	S3
	Planum polare of the superior temporal gyrus R	(3.16, 0.005)	S2
	Inferior temporal gyrus L	(3.53, 0.002)	S4
	Middle temporal gyrus L	(3.02, 0.007)	S4
	Posterior ramus (or segment) of the lateral sulcus (or fissure) R	(3.29, 0.004)	S2

Table S2: List of ROIs that show a significant condition effect at least once during the training in the MEG modality ($p < 0.021$).

Frequency bands	ROI	(t, p)	Session
α_1	Paracentral lobule and sulcus L	(2.90, 0.009)	S2
	Cuneus L	(-3.19, 0.005)	S4
	Opercular part of the inferior frontal gyrus L	(3.84, 0.001)	S2
	Short insular gyri L	(2.59, 0.018)	S4
	Supramarginal gyrus L	(3.07, 0.006)	S1
	Anterior transverse temporal gyrus L	(2.71, 0.014)	S4
	Horizontal ramus of the anterior segment of the lateral sulcus R	(2.68, 0.015)	S4
	Vertical ramus of the anterior segment of the lateral sulcus L	(2.68, 0.015)	S2
	Middle-Anterior part of the cingulate gyrus and sulcus L	(-2.70, 0.014)	(S2)
α_2	Cuneus L	(-2.62, 0.017)	S3
	Triangular part of the inferior frontal gyrus R	(2.89, 0.009)	S3
	Supramarginal gyrus L	(2.59, 0.018)	S3
	Orbital part of the inferior frontal gyrus L	(2.64, 0.016)	S3
β_1	Orbital part of the inferior frontal gyrus R	(-2.57, 0.019)	S3
	Lateral occipito-temporal gyrus L	(3.27, 0.004)	S3
	Transverse frontopolar gyri and sulci R	(-2.86, 0.010)	S3
β_2	Posterior-ventral part of the cingulate gyrus L	(-3.10, 0.006)	S1
	Orbital part of the inferior frontal gyrus R	(-2.67, 0.015)	S4
	Lateral occipito-temporal gyrus L	(2.56, 0.019)	S3
	Postcentral gyrus R	(-2.72, 0.014)	S2
	Planum polare of the superior temporal gyrus R	(-2.64, 0.016)	S1

Table S3: List of ROIs that show a significant condition effect at least once during the training in the mux modality ($p < 0.021$).

Frequency bands	ROI	(t, p)	Session
α_1	Anterior part of the cingulate gyrus and sulcus L	(2.64, 0.016)	S3
	Middle-posterior part of the cingulate gyrus and sulcus L	(-2.71, 0.014)	S2
	Transverse frontopolar gyri and sulci R	(2.86, 0.010)	S1
	Posterior-dorsal part of the cingulate gyrus R	(-3.01, 0.007)	S2
	Opercular part of the inferior frontal gyrus L	(2.53, 0.020)	S4
	Superior occipital gyrus L	(-2.60, 0.017)	S1
	Precuneus L	(-3.43, 0.003)	S2
	Gyrus rectus L	(2.63, 0.017)	S4
	Anterior transverse temporal gyrus L	(2.53, 0.020)	S4
	Planum polare of the superior temporal gyrus L	(2.78, 0.012)	S4
	α_2	Long insular gyrus and central sulcus of the insula R	(3.09, 0.006)
Middle-posterior part of the cingulate gyrus and sulcus L		(2.79, 0.012)	S4
Subcentral gyrus L		(2.54, 0.020)	S4
Cuneus R		(-2.60, 0.018)	S1
Superior parietal lobule L		(-2.87, 0.010)	S2
Precuneus L		(-2.64, 0.016)	S2
Gyrus rectus L		(2.62, 0.017; 2.97, 0.008)	(S3; S4)
Gyrus rectus R		(2.65, 0.016)	S3
Planum temporale or temporal plane of the superior temporal gyrus L		(2.37, 0.029)	S4
Middle temporal gyrus L		(-2.45, 0.024)	S2
β_1		Orbital part of the inferior frontal gyrus R	(-3.41, 0.003)
	Short insular gyri R	(2.85, 0.010)	S1
	Lateral occipito-temporal gyrus R	(2.56, 0.019)	S3
	Gyrus rectus R	(2.72, 0.014)	S1
	Planum polare of the superior temporal gyrus L	(2.72, 0.014)	S1
β_2	Posterior-ventral part of the cingulate gyrus L	(2.76, 0.012)	S2
	Posterior-ventral part of the cingulate gyrus R	(3.33, 0.004)	S2
	Opercular part of the inferior frontal gyrus L	(-2.62, 0.017)	S1
	Lateral occipito-temporal gyrus R	(2.89, 0.009)	S3
	Occipital pole R	(2.58, 0.019)	S2